J. Chem. Thermodynamics 88 (2015) 44–60

Contents lists available at ScienceDirect

J. Chem. Thermodynamics

journal homepage: www.elsevier.com/locate/jct

# Volumetric and acoustical properties of aqueous mixtures of N-methyl-2-hydroxyethylammonium propionate at $T = (298.15$ to $333.15)$ K

Yang Li [a], Eduardo J.P. Figueiredo [b], Mário J.S.F. Santos [b], Jaime B. Santos [b], Nieves M.C. Talavera-Prieto [c], Pedro J. Carvalho [d], Abel G.M. Ferreira [c,*], Silvana Mattedi [e]

[a] Shanghai Key Laboratory of Modern Metallurgy & Materials Processing, Shanghai University, Yanchang Road, 200072 Shanghai, China
[b] Department of Electrical and Computers Engineering, University of Coimbra, Polo II, Rua Silvio Lima, 3030-970 Coimbra, Portugal
[c] Department of Chemical Engineering, University of Coimbra, Polo II, Rua Silvio Lima, 3030-970 Coimbra, Portugal
[d] CICECO, Departamento de Química, Universidade de Aveiro, 3810-193 Aveiro, Portugal
[e] Escola Politécnica, Universidade Federal da Bahia, Rua Aristides Novis 2, Federação, 40210-630 Salvador, Bahia, Brazil

ARTICLE INFO

*Article history:*
Received 1 December 2014
Received in revised form 30 March 2015
Accepted 3 April 2015
Available online 8 April 2015

*Keywords:*
Ionic liquid
Density
Jouyban–Acree model
Padé approximant
Speed of sound
Apparent molar volume
Apparent molar isentropic compressibility

ABSTRACT

The speed of sound in the ionic liquid (IL) N-methyl-2-hydroxyethylammonium propionate (m2HEAPr) was measured at atmospheric pressure, and over the range of temperatures $T = (293.15$ to $343.15)$ K. The speed of sound and density were also measured for aqueous mixtures of the ionic liquid throughout the entire concentration range at temperatures $T = (298.15$ to $333.15)$ K and atmospheric pressure. The excess molar volume, excess isentropic compressibility, excess speed of sound, apparent molar volume, and isentropic apparent molar compressibility were calculated from the values of the experimental density and speed of sound. The results were analyzed and are discussed from the point of view of structural changes in the aqueous medium. All the above mentioned properties were correlated with selected analytical functions. The Jouyban–Acree model was used to correlate the density of the mixtures studied with the temperature. The model accuracy was evaluated by calculating the absolute average deviation (*AAD*) for the correlation, which is 0.4%. The speed of sound of the m2HEAPr was predicted with the Wu *et al.* model with a maximum deviation of 2%. The molar compressibility of m2HEAPr and their aqueous mixtures was calculated from the Wada's model. To the authors' knowledge, this is the first time this model is applied to these systems. The results demonstrate that the molar compressibility calculated from Wada's model is almost a linear function of mole fraction and can be considered as temperature independent for a fixed mole fraction over the whole composition range.



## 1. Introduction

Due to their very low vapour pressures, the contribution of ILs for air pollution is negligible. However, ILs may have a significant solubility in water. Therefore, they may contaminate water streams, leading to environmental problems. Once in the environment, the IL ecotoxicity depends directly on their lipophilicity [1–3]. Therefore the knowledge of the ILs solubility in water can be an effective way to predict their toxicity in ecosystems. Furthermore, the knowledge of thermophysical properties of water and hydrophilic IL mixtures is required for the development of practical applications and design of processes using (water + IL) systems.

The ionic liquids from substituted hydroxyethylammonium cations and organic acid anions can be obtained by simple synthesis [4,5], and have important applications [6]. Moreover, it was verified that some ILs of that family present a negligible toxicity [7].

Among several thermodynamic properties, the volumetric and acoustical properties are very important for design and theoretical studies. For instance, the knowledge of the excess molar volume, isentropic compressibility, and apparent molar properties is essential to develop reliable predictive models [8,9], as well as to understand the nature of (solute + solvent) and (solute + solute) interactions.

Some previous studies have shown that the addition of even small amounts of water can significantly influence the ionic liquids density and the speed of sound [10]. The studies for ILs aqueous systems includes three kinds of approaches: the report on property values for dilute aqueous solutions of ILs [9,11–17], the

* Corresponding author. Tel.: +351 239 798 729; fax: +351 239 798 703.
*E-mail addresses:* abel@eq.uc.pt, fabel7@gmail.com (A.G.M. Ferreira).

http://dx.doi.org/10.1016/j.jct.2015.04.005
0021-9614/

investigation of the effect of water content in pure ILs [10,18–32], and the measurements covering the whole composition range [5,33–59]. The density and speed of sound measurements for hydroxyethylammonium (HEA) cation based ILs with organic acid anions mixed with solvents are scarce and were reported by Iglesias *et al.* [5] for mixtures of 2-hydroxyethylammonium formate with short hydroxylic solvents (water, methanol and ethanol) and Álvarez *et al.* [59] for mixtures of 2-hydroxyethylammonium acetate with the same solvents. The density of hydroxyethylammonium (HEA) cation based ILs with organic acid anions was presented by Kurnia *et al.* for mixtures involving 2-hydroxyethylammonium formate, acetate, propionate, and lactate with methanol [60], mixtures of bis(2-hydroxyethyl)methylammonium formate and acetate with alcohols [61,62], and Taib and Murugesan [63] made measurements for aqueous mixtures of bis(2-hydroxyethyl)ammonium acetate. An excellent survey about the physical properties of ILs binary mixtures with water and ethanol was performed by Cabeza *et al.* [64].

In this work, the experimental measurements of the speed of sound for m2HEAPr at temperatures ranging from (293.15 to 343.15) K and 102.2 kPa are given. For aqueous solutions of m2HEAPr, the speed of sound and the density over all concentration ranges at temperatures from (298.15 to 333.15) K were measured. These results were used to obtain important derived properties to include the isentropic compressibility ($k_S$), the IL apparent molar volume ($V\phi$) and compressibility ($k\phi$), excess molar volume, isentropic compressibility, and speed of sound. All these properties were successfully represented by analytical functions applied over the concentration and temperature ranges of measurements. Values of the limiting apparent molar volume and isentropic compressibility of ILs were evaluated and examined to study the effect of the (IL + water) and (IL + IL) interactions.

## 2. Experimental

Water (mili-Q) was used for preparation of the aqueous solutions. The preparation of N-methyl-2-hydroxyethylammonium propionate was described in detail by Talavera-Prieto *et al.* [6]. The water content in the IL was determined with a Metrohm 831 Karl Fisher coulometer indicating a water mass fraction lower than $3 \cdot 10^{-4}$. The mixtures (IL + water) were prepared by mass using a Mettler AT 200 balance with an uncertainty of $\pm 10^{-5}$ g. The uncertainty in the mole fraction was estimated as being about $\pm 10^{-4}$. Table 1 summarizes relevant information on sample material purities.

The densities were measured using an Anton Paar DMA 60 digital vibrating tube densimeter, with a DMA 512P measuring cell. The measuring setup and the vibrating tube densimeter calibration were described in a recent work with detail [65]. The expected uncertainty for density due to viscosity of the ionic liquid and its aqueous solutions (damping effects on the vibrating tube) was $0.3\ \mathrm{kg \cdot m^{-3}}$ maximum for the studied range of temperatures [65]. The uncertainties in temperature, $T$, and pressure, $p$, were $u(T) = \pm 0.02$ K and $u(p) = \pm 0.02$ MPa, respectively. The combined standard uncertainty of the density measurements, $\rho$, estimated taking into account the influence of uncertainties associated with the calibration equation [65], temperature, pressure, period of oscillations (six-digit frequency counter), viscosity, and calibrating fluids density data, was $u(\rho) = \pm 0.86\ \mathrm{kg \cdot m^{-3}}$.

**TABLE 1**
Provenance and mass fraction purity of the materials studied.

| Chemical | Supplier (CAS N) | Mass fraction purity[a] | |
|---|---|---|---|
| | | As received | Water content |
| 2-Methylaminoethanol | Sigma–Aldrich (109-83-1) | 0. 99 | |
| Propanoic acid | Sigma–Aldrich (79-09-4) | >0.995 | |
| m2HEAPr | | >0.99 | $3 \cdot 10^{-4}$ |

[a] The m2HEAPr was fully distilled under high vacuum ($10^{-4}$ Pa) and the distillate mass fraction purity checked by $^1$H NMR and $^{13}$C NMR is higher than 0.99. The final water content was determined with a Metrohm 831 Karl Fisher coulometer.

For the measurement of the speed of sound a stainless steel cell has been built and assembled in our laboratory. Two 5 MHz ultrasonic transducers (one acting as a transmitter and the other as a receiver) were mounted in cavities drilled on its plane surfaces. The ultrasound wave propagation time corresponding to the path between the transmitter and receiver was collected and displayed by an oscilloscope, and then transferred to a computer for processing. The time of flight in the mixture, ($\triangle\tau$), was obtained subtracting the time of the emitter-receiver path from the propagation time in the steel walls. The cell was calibrated by measuring $\triangle\tau$ in water, toluene, and 1,2-butandiol at atmospheric pressure. The measuring setup and the cell calibration were described with detail in a previous paper [66]. The combined standard uncertainty in the speed of sound measurement was $u(u) = \pm 1.2\ \mathrm{m \cdot s^{-1}}$.

The density and speed of sound measurements of the binary mixtures were made with the DMA 512P and speed of sound measuring cells open to the atmosphere. The measurement of the atmospheric pressure was made using a calibrated pressure transducer (AFRISO Euro-Index, DMU03). Taking the observed values covering February and March the mean value was $p = (102.24 \pm 0.39)$ kPa.

## 3. Results and discussion

### 3.1. Properties of pure substances

The experimental values are presented in table 2 for the density and speed of sound in water and m2HEAPr at atmospheric pressure within the range $T = (293.15$ to $333.15)$ K together with the molar volume, $V_m$, and the isentropic compressibility, $k_S$. The molar volumes can be calculated from density using the expression showed in equation (1):

$$V_m = \frac{M}{\rho}, \tag{1}$$

where $M$ is the molar mass of pure water or IL.

The isentropic compressibility defined by equation (2)

$$k_S = -\frac{1}{V_m}\left(\frac{\partial V_m}{\partial p}\right)_S = \frac{1}{\rho}\left(\frac{\partial \rho}{\partial p}\right)_S = \left(\frac{\partial \ln \rho}{\partial p}\right)_S, \tag{2}$$

where $S$ is the entropy, was calculated from the Laplace–Newton's equation (equation (3)):

$$k_s = \frac{1}{\rho u^2}, \tag{3}$$

where $u$ is the speed of sound.

For water density, values from NIST [67] have been used, whereas for m2HEAPr the values were taken from a previous work [6]. For these substances, the density and the molar volume behave as expected, *i.e.*, the density decreases and the molar volume increases as temperature increases. Concerning the speed of sound, it increases in water and decreases in the ionic liquid at increasing temperatures. As a result, the isentropic compressibility decreases for water and increases for m2HEAPr. Although the ionic liquid has a lower isentropic compressibility than water, the value of this property is nearly the same for the two substances at $T = 333.15$ K.

In table 2, the isobaric molar heat capacity $C_{p,m}$ is also reported. The values were extracted from NIST [67] for water and from the empirical equation given in [6] for the m2HEAPr.

**TABLE 2**
Density, $\rho$, molar volume $V_m$, speed of sound $u$, isentropic compressibility $k_S$, isobaric molar heat capacity $C_{p,m}$, and thermal expansivity $\alpha_p$ of pure water and m2HEAPr at several temperatures and $p$ = 0.102 MPa.

| $T$/K | $\rho$/(kg · m$^{-3}$) | $V_m$/(cm$^3$ · mol$^{-1}$) | $u$/(m · s) | $10^{10}\kappa_s$/(Pa$^{-1}$) | $C_{p,m}$/(J · K$^{-1}$ · mol$^{-1}$) | $10^4\alpha_p$/(K$^{-1}$) |
|---|---|---|---|---|---|---|
| | | | *Water* | | | |
| 298.15 | 997.1[a] | 18.068 | 1496.7[a] | 4.477 | 75.33[d] | 2.572[b] |
| 303.15 | 995.7[a] | 18.094 | 1509.2[a] | 4.410 | 75.30[d] | 3.030[a] |
| 308.15 | 994.0[a] | 18.123 | 1519.8[a] | 4.355 | 75.29[d] | 3.457[b] |
| 313.15 | 992.2 [a] | 18.156 | 1528.9[a] | 4.312 | 75.29[d] | 3.853[b] |
| 318.15 | 990.2[a] | 18.193 | 1536.4[a] | 4.278 | 75.31[d] | 4.225[b] |
| 323.15 | 988.0[a] | 18.233 | 1542.6[a] | 4.253 | 75.33[d] | 4.576[b] |
| 328.15 | 985.7[a] | 18.277 | 1547.4[a] | 4.237 | 75.36[d] | 4.911[b] |
| 333.15 | 983.2[a] | 18.323 | 1551.0[a] | 4.228 | 75.39[d] | 5.231[b] |
| | | | *m2HEAPr* | | | |
| 293.15[e] | | | 1656.9 | | 325.92[d] | 5.852 |
| 298.15 | 1065.8[c] | 139.984 | 1638.4 | 3.495 | 327.47[d] | 5.907 |
| 303.15 | 1062.6[c] | 140.400 | 1624.6 | 3.565 | 329.01[d] | 5.962 |
| 308.15 | 1059.4[c] | 140.822 | 1607.0 | 3.655 | 330.56[d] | 6.018 |
| 313.15 | 1056.2[c] | 141.248 | 1588.5 | 3.752 | 332.10[d] | 6.074 |
| 318.15 | 1053.0[c] | 141.680 | 1573.2 | 3.837 | 333.65[d] | 6.129 |
| 323.15 | 1049.8[c] | 142.116 | 1558.3 | 3.923 | 335.20[d] | 6.185 |
| 328.15 | 1046.5[c] | 142.559 | 1543.7 | 4.010 | 336.74[d] | 6.241 |
| 333.15 | 1043.2[c] | 143.006 | 1527.0 | 4.111 | 338.29[d] | 6.296 |
| 338.15 | 1039.9[c] | 143.464 | 1507.1 | 4.234 | 339.83[d] | 6.353 |
| 343.15 | 1036.6[c] | 143.918 | 1492.6 | 4.330 | 341.38[d] | 6.409 |

$u(p)$ < ±0.39 kPa.
For m2HEAPr, standard uncertainties $u(\rho)$ = ±0.86 kg · m$^{-3}$, $u(u)$ = ±1.2 m · s$^{-1}$.
[a] From NIST [67].
[b] From Chen *et al.* [68].
[c] Experimental data by Talavera-Prieto *et al.* [6].
[d] From $C_{p,m}$/(J · K$^{-1}$ · mol$^{-1}$) = 235.31 + 0.3091($T$/K) [6].
[e] $u(T)$ = ±0.02 K.

The thermal expansivity, $\alpha_p$, of pure substances is required for calculating the excess properties of the (m2HEAPr + $H_2O$) mixtures. The thermal expansivity is defined by equation (4)

$$\alpha_p = \frac{1}{V_m}\left(\frac{\partial V_m}{\partial T}\right)_p = -\frac{1}{\rho}\left(\frac{\partial \rho}{\partial T}\right)_p = -\left(\frac{\partial \ln \rho}{\partial T}\right)_p. \quad (4)$$

For water, the thermal expansivity values reported by Chen *et al.* [68] were used. For m2HEAPr the polynomial

$$\ln(\rho/\text{kg}\cdot\text{m}^{-3}) = 7.0981 - 2.5882\cdot 10^{-4}(T/\text{K}) - 5.5669\cdot 10^{-7}(T/\text{K})^2 \quad (5)$$

was found to correlate well the density variation with temperature at atmospheric pressure with a standard deviation in density almost zero. From equation (5) combined with equation (4), the thermal expansivity of the ionic liquid was calculated for the temperature values given in table 2. These values agree within 2.8% with the ones derived from density measurements made by Alvarez *et al.* [69].

### 3.2. Volumetric properties of liquid mixtures

The densities of pure methyl-2-hydroxyethylammonium propionate (m2HEAPr) were measured by the authors in a previous work [6] over the ranges $T$ = (298.15 to 358.15) K and $p$ = (0.1 to 25) MPa. The results at atmospheric pressure will be used in the calculations that follow. The measured density values for temperatures (298.15 to 333.15) K considering the binary mixtures of the IL with water as function of the mole fraction are presented in table 3. The experimental density values were correlated using the Jouyban–Acree model [70] (equation (6))

$$\ln \rho = x_1 \ln \rho_1 + x_2 \ln \rho_2 + x_1x_2\sum_{i=0}^{2}\frac{C_i(x_1 - x_2)^i}{T}, \quad (6)$$

where $\rho_1$, $\rho_2$ are the densities of IL and water at temperature $T$, respectively, and the $C_i$s represents the model parameters [70,71] that were calculated by regressing ($\ln\rho - x_1\ln\rho_1 - x_2\ln\rho_2$) against $x_1x_2/T$, $x_1x_2(x_1 - x_2)/T$, and $x_1x_2(x_1 - x_2)^2/T$, using a non-intercept least square analysis [72]. The parameters $C_i$s are presented in table 4. Values of the density are represented over the whole temperature and composition ranges with standard deviation of 4.5 kg · m$^{-3}$, which corresponds to an *AAD* of 0.38%. The relative deviations between the calculated and experimental densities are shown in figure 1.

For some mixtures having the same composition, the deviations spread out over a large range as temperature changes, reaching important values: at $x_1$ = 0.02 the relative deviation ranges between −0.54% at $T$ = 298.15 K and 0.28% at $T$ = 333.15 K. This behaviour might be due to the simple analytical description of ln $\rho$ on temperature by equation (6). To improve the accuracy of the density correlation the ($T$,$x$) part has been described using the rational functions (Padé approximant),

$$\ln \rho = x_1 \ln \rho_1 + x_2 \ln \rho_2 + x_1x_2\frac{\sum_{i=0}^{m}C_i(2x_1 - 1)^i}{1 + \sum_{i=1}^{n}D_i(2x_1 - 1)^i} \quad (7)$$

applied to a specific temperature, where $C_i(T)$ and $D_i(T)$ are adjustable temperature dependent coefficients. Equation (7) enables a large number of possible fittings because the adjustable coefficients in each polynomial term can be different, with a total of k = (m + n + 1) for fitting at a fixed temperature. However, in this work the coefficients of equation (7) were obtained by fitting to the density using simultaneously the temperatures and compositions in the whole ranges. The $C_i$ and $D_i$ were expressed by linear equations on temperature:

$$C_i = C_{i,0} + C_{i,1}T, \quad (8)$$

$$D_i = D_{i,0} + D_{i,1}T. \quad (9)$$

This procedure can lead to coefficients reduction of (t × k) to (2 × k) where t is the number of different temperatures tested. Equation (7) is a new model proposed to represent density of binary mixtures. The parameters $C_{ij}$ and $D_{ij}$ (j = 0,1) of equation (8) and

**TABLE 3**
Density, $\rho$, speed of sound $u$, excess molar volume $V_m^E$, isentropic compressibility $k_S$, molar compressibility $k_m$, excess isentropic compressibility, $k_S^E$, excess speed of sound $u^E$, apparent molar volume $V_\phi$, and apparent molar compressibility $k_\phi$, for the binary system m2HEAPr(1) + $H_2O$(2) at $p$ = 0.102 MPa.

| $x_1$[a] | $m_{IL}$[b]/ (mol · kg$^{-1}$) | ρ[c]/ (kg · m$^{-3}$) | u[d]/ (m · s$^{-1}$) | $V^E$[e]/ (cm$^3$ · mol$^{-1}$) | $10^{10}\kappa_S$[f]/ (Pa$^{-1}$) | $10^4 k_m$[g]/ (m$^3$ · mol$^{-1}$ · Pa$^{1/7}$) | $10^{10}k_S^E$/ (Pa$^{-1}$) | $u^E$/ (m · s$^{-1}$) | $V_\phi$[h]/ (cm$^3$ · mol$^{-1}$) | $10^{14}k_\phi$[i]/ (m$^3$ · mol$^{-1}$ · Pa$^{-1}$) |
|---|---|---|---|---|---|---|---|---|---|---|
| | | | | | *298.15* | | | | | |
| 0.0000 | 0.00 | 997.1 | 1496.7 | 0.000 | 4.477 | 3.913 | 0.000 | 0.0 | | |
| 0.0200 | 1.13 | 1016.8 | 1628.3 | −0.209 | 3.709 | 4.515 | −0.666 | 121.3 | 129.54 | −2.01 |
| 0.0501 | 2.93 | 1039.1 | 1746.5 | −0.514 | 3.155 | 5.387 | −1.097 | 225.9 | 129.75 | −0.42 |
| 0.1001 | 6.17 | 1056.2 | 1820.9 | −0.784 | 2.855 | 6.810 | −1.247 | 281.6 | 132.16 | 1.14 |
| 0.1010 | 6.23 | 1055.8 | 1818.1 | −0.771 | 2.865 | 6.835 | −1.234 | 278.5 | 132.34 | 1.20 |
| 0.2006 | 13.9 | 1072.5 | 1827.2 | −1.194 | 2.793 | 9.575 | −1.116 | 260.7 | 134.02 | 2.53 |
| 0.3010 | 23.9 | 1072.6 | 1790.1 | −1.157 | 2.909 | 12.347 | −0.880 | 204.8 | 136.14 | 3.30 |
| 0.3978 | 36.7 | 1074.0 | 1757.0 | −1.207 | 3.016 | 14.976 | −0.695 | 158.4 | 136.95 | 3.73 |
| 0.4976 | 55.0 | 1072.3 | 1726.2 | −1.064 | 3.130 | 17.703 | −0.521 | 117.1 | 137.85 | 4.07 |
| 0.5972 | 82.3 | 1071.9 | 1721.0 | −0.985 | 3.150 | 20.469 | −0.456 | 103.6 | 138.34 | 4.20 |
| 0.8006 | 222.9 | 1068.7 | 1684.5 | −0.546 | 3.298 | 26.045 | −0.242 | 54.7 | 139.30 | 4.54 |
| 1.0000 | | 1065.8 | 1638.4 | 0.000 | 3.496 | 31.405 | 0.000 | 0.0 | | |
| | | | | | *303.15* | | | | | |
| 0.0000 | 0.00 | 995.7 | 1509.2 | 0.000 | 4.410 | 3.927 | 0.000 | 0.0 | | |
| 0.0200 | 1.13 | 1013.4 | 1630.6 | −0.174 | 3.711 | 4.530 | −0.612 | 113.4 | 131.70 | −1.32 |
| 0.0501 | 2.93 | 1036.3 | 1741.6 | −0.495 | 3.181 | 5.395 | −1.038 | 213.7 | 130.55 | −0.06 |
| 0.1001 | 6.17 | 1053.4 | 1810.8 | −0.771 | 2.895 | 6.814 | −1.197 | 267.9 | 132.70 | 1.38 |
| 0.1010 | 6.23 | 1052.8 | 1807.0 | −0.752 | 2.909 | 6.839 | −1.181 | 263.8 | 132.95 | 1.45 |
| 0.2006 | 13.9 | 1069.5 | 1812.4 | −1.182 | 2.846 | 9.576 | −1.079 | 247.3 | 134.50 | 2.70 |
| 0.3010 | 23.9 | 1069.5 | 1775.9 | −1.145 | 2.965 | 12.349 | −0.858 | 195.3 | 136.60 | 3.44 |
| 0.3978 | 36.7 | 1070.9 | 1742.3 | −1.201 | 3.076 | 14.976 | −0.678 | 150.7 | 137.38 | 3.86 |
| 0.4976 | 55.0 | 1069.2 | 1711.0 | −1.058 | 3.195 | 17.702 | −0.507 | 110.7 | 138.28 | 4.20 |
| 0.5972 | 82.3 | 1068.7 | 1705.5 | −0.981 | 3.217 | 20.468 | −0.445 | 98.3 | 138.76 | 4.32 |
| 0.8006 | 222.9 | 1065.4 | 1668.3 | −0.536 | 3.372 | 26.040 | −0.231 | 50.7 | 139.73 | 4.67 |
| 1.0000 | | 1062.6 | 1624.6 | 0.000 | 3.565 | 31.410 | 0.000 | 0.0 | | |
| | | | | | *308.15* | | | | | |
| 0.0000 | 0.00 | 994.0 | 1519.8 | 0.000 | 4.355 | 3.940 | 0.000 | 0.0 | | |
| 0.0200 | 1.13 | 1010.0 | 1632.8 | −0.143 | 3.714 | 4.545 | −0.573 | 107.8 | 133.61 | −0.75 |
| 0.0501 | 2.93 | 1033.5 | 1736.7 | −0.480 | 3.208 | 5.403 | −0.995 | 204.2 | 131.25 | 0.27 |
| 0.1001 | 6.17 | 1050.7 | 1800.7 | −0.762 | 2.935 | 6.819 | −1.163 | 257.3 | 133.19 | 1.59 |
| 0.1010 | 6.23 | 1049.9 | 1795.9 | −0.737 | 2.953 | 6.844 | −1.143 | 252.3 | 133.51 | 1.68 |
| 0.2006 | 13.9 | 1066.5 | 1797.6 | −1.173 | 2.902 | 9.576 | −1.059 | 237.4 | 134.96 | 2.86 |
| 0.3010 | 23.9 | 1066.4 | 1761.6 | −1.137 | 3.022 | 12.351 | −0.852 | 189.5 | 137.04 | 3.58 |
| 0.3978 | 36.7 | 1067.9 | 1727.6 | −1.199 | 3.138 | 14.977 | −0.678 | 146.8 | 137.81 | 3.99 |
| 0.4976 | 55.0 | 1066.1 | 1695.7 | −1.054 | 3.262 | 17.701 | −0.509 | 108.1 | 138.70 | 4.32 |
| 0.5972 | 82.3 | 1065.6 | 1689.9 | −0.980 | 3.286 | 20.466 | −0.452 | 96.8 | 139.18 | 4.44 |
| 0.8006 | 222.9 | 1062.2 | 1652.0 | −0.529 | 3.450 | 26.035 | −0.239 | 50.7 | 140.16 | 4.79 |
| 1.0000 | | 1059.4 | 1607.0 | 0.000 | 3.655 | 31.393 | 0.000 | 0.0 | | |
| | | | | | *313.15* | | | | | |
| 0.0000 | 0.00 | 992.2 | 1528.9 | 0.000 | 4.312 | 3.953 | 0.000 | 0.0 | | |
| 0.0200 | 1.13 | 1006.6 | 1635.1 | −0.115 | 3.716 | 4.560 | −0.544 | 103.8 | 135.45 | −0.28 |
| 0.0501 | 2.93 | 1030.6 | 1731.8 | −0.467 | 3.235 | 5.412 | −0.961 | 196.4 | 131.92 | 0.56 |
| 0.1001 | 6.17 | 1047.9 | 1790.6 | −0.757 | 2.976 | 6.823 | −1.139 | 248.5 | 133.68 | 1.80 |
| 0.1010 | 6.23 | 1046.9 | 1784.7 | −0.725 | 2.999 | 6.848 | −1.115 | 242.5 | 134.06 | 1.90 |
| 0.2006 | 13.9 | 1063.5 | 1782.8 | −1.168 | 2.958 | 9.577 | −1.046 | 229.2 | 135.42 | 3.02 |
| 0.3010 | 23.9 | 1063.3 | 1747.4 | −1.132 | 3.080 | 12.353 | −0.854 | 185.2 | 137.49 | 3.72 |
| 0.3978 | 36.7 | 1064.8 | 1712.8 | −1.200 | 3.201 | 14.977 | −0.685 | 144.2 | 138.23 | 4.12 |
| 0.4976 | 55.0 | 1063.0 | 1680.5 | −1.054 | 3.331 | 17.700 | −0.518 | 106.7 | 139.13 | 4.46 |
| 0.5972 | 82.3 | 1062.5 | 1674.4 | −0.982 | 3.357 | 20.463 | −0.464 | 96.5 | 139.60 | 4.57 |
| 0.8006 | 222.9 | 1059.0 | 1635.7 | −0.525 | 3.529 | 26.029 | −0.251 | 51.6 | 140.59 | 4.93 |
| 1.0000 | | 1056.2 | 1588.5 | 0.000 | 3.752 | 31.370 | 0.000 | 0.0 | | |
| | | | | | *318.15* | | | | | |
| 0.0000 | 0.00 | 990.2 | 1536.4 | 0.000 | 4.278 | 3.965 | 0.000 | 0.0 | | |
| 0.0200 | 1.13 | 1003.2 | 1637.4 | −0.090 | 3.718 | 4.575 | −0.523 | 101.0 | 137.13 | 0.09 |
| 0.0501 | 2.93 | 1027.8 | 1726.9 | −0.459 | 3.262 | 5.420 | −0.932 | 189.3 | 132.53 | 0.82 |
| 0.1001 | 6.17 | 1045.2 | 1780.5 | −0.755 | 3.018 | 6.827 | −1.114 | 239.7 | 134.13 | 1.99 |
| 0.1010 | 6.23 | 1043.9 | 1773.6 | −0.717 | 3.045 | 6.853 | −1.086 | 232.7 | 134.57 | 2.10 |
| 0.2006 | 13.9 | 1060.5 | 1768.0 | −1.166 | 3.017 | 9.577 | −1.028 | 220.1 | 135.86 | 3.18 |
| 0.3010 | 23.9 | 1060.2 | 1733.1 | −1.130 | 3.140 | 12.355 | −0.848 | 179.3 | 137.92 | 3.85 |
| 0.3978 | 36.7 | 1061.8 | 1698.1 | −1.204 | 3.266 | 14.978 | −0.683 | 139.7 | 138.66 | 4.25 |
| 0.4976 | 55.0 | 1059.8 | 1665.2 | −1.056 | 3.403 | 17.700 | −0.516 | 103.1 | 139.56 | 4.59 |
| 0.5972 | 82.3 | 1059.4 | 1658.8 | −0.987 | 3.430 | 20.460 | −0.465 | 93.7 | 140.03 | 4.70 |
| 0.8006 | 222.9 | 1055.8 | 1619.5 | −0.524 | 3.611 | 26.023 | −0.249 | 49.6 | 141.03 | 5.06 |
| 1.0000 | | 1053.0 | 1573.2 | 0.000 | 3.837 | 31.370 | 0.000 | 0.0 | | |
| | | | | | *323.15* | | | | | |
| 0.0000 | 0.00 | 988.0 | 1542.6 | 0.000 | 4.253 | 3.978 | 0.000 | 0.0 | | |
| 0.0200 | 1.13 | 999.8 | 1639.6 | −0.069 | 3.720 | 4.590 | −0.510 | 99.4 | 138.64 | 0.39 |
| 0.0501 | 2.93 | 1025.0 | 1722.0 | −0.453 | 3.290 | 5.428 | −0.908 | 183.3 | 133.07 | 1.05 |
| 0.1001 | 6.17 | 1042.4 | 1770.4 | −0.756 | 3.060 | 6.832 | −1.094 | 231.7 | 134.55 | 2.16 |

(*continued on next page*)

**TABLE 3** (*continued*)

| $x_1$[a] | $m_{IL}$[b]/ (mol · kg$^{-1}$) | ρ[c]/ (kg · m$^{-3}$) | u[d]/ (m · s$^{-1}$) | $V^E$[e]/ (cm$^3$ · mol$^{-1}$) | $10^{10}\kappa_s$[f]/ (Pa$^{-1}$) | $10^4 k_m$[g]/ (m$^3$ · mol$^{-1}$ · Pa$^{1/7}$) | $10^{10}k_S^E$/ (Pa$^{-1}$) | $u^E$/ (m · s$^{-1}$) | $V_\phi$[h]/ (cm$^3$ · mol$^{-1}$) | $10^{14}k_\phi$[i]/ (m$^3$ · mol$^{-1}$ · Pa$^{-1}$) |
|---|---|---|---|---|---|---|---|---|---|---|
| 0.1010 | 6.23 | 1040.9 | 1762.5 | −0.711 | 3.093 | 6.857 | −1.061 | 223.8 | 135.06 | 2.29 |
| 0.2006 | 13.9 | 1057.5 | 1753.2 | −1.166 | 3.077 | 9.577 | −1.013 | 211.5 | 136.29 | 3.34 |
| 0.3010 | 23.9 | 1057.1 | 1718.9 | −1.131 | 3.202 | 12.357 | −0.843 | 173.8 | 138.36 | 3.98 |
| 0.3978 | 36.7 | 1058.7 | 1683.3 | −1.210 | 3.333 | 14.977 | −0.681 | 135.4 | 139.07 | 4.38 |
| 0.4976 | 55.0 | 1056.7 | 1650.0 | −1.061 | 3.476 | 17.697 | −0.514 | 99.5 | 139.98 | 4.72 |
| 0.5972 | 82.3 | 1056.2 | 1643.3 | −0.994 | 3.506 | 20.457 | −0.465 | 90.7 | 140.45 | 4.83 |
| 0.8006 | 222.9 | 1052.6 | 1603.2 | −0.525 | 3.696 | 26.016 | −0.246 | 47.3 | 141.46 | 5.20 |
| 1.0000 | | 1049.8 | 1558.3 | 0.000 | 3.923 | 31.363 | 0.000 | 0.0 | | |
| | | | | | | *328.15* | | | | |
| 0.0000 | 0.00 | 985.7 | 1547.4 | 0.000 | 4.237 | 3.989 | 0.000 | 0.0 | | |
| 0.0200 | 1.13 | 996.4 | 1641.9 | −0.049 | 3.723 | 4.605 | −0.503 | 99.1 | 140.071 | 0.60 |
| 0.0501 | 2.93 | 1022.2 | 1717.1 | −0.451 | 3.318 | 5.437 | −0.892 | 178.4 | 133.577 | 1.25 |
| 0.1001 | 6.17 | 1039.7 | 1760.3 | −0.760 | 3.104 | 6.836 | −1.078 | 224.7 | 134.959 | 2.33 |
| 0.1010 | 6.23 | 1037.9 | 1751.4 | −0.708 | 3.141 | 6.862 | −1.041 | 215.7 | 135.539 | 2.47 |
| 0.2006 | 13.9 | 1054.5 | 1738.3 | −1.170 | 3.138 | 9.577 | −0.999 | 203.5 | 136.716 | 3.49 |
| 0.3010 | 23.9 | 1054.0 | 1704.6 | −1.136 | 3.265 | 12.358 | −0.840 | 168.6 | 138.786 | 4.12 |
| 0.3978 | 36.7 | 1055.6 | 1668.6 | −1.220 | 3.402 | 14.976 | −0.679 | 131.2 | 139.493 | 4.52 |
| 0.4976 | 55.0 | 1053.6 | 1634.8 | −1.070 | 3.552 | 17.695 | −0.511 | 95.9 | 140.410 | 4.86 |
| 0.5972 | 82.3 | 1053.1 | 1627.8 | −1.005 | 3.584 | 20.453 | −0.464 | 87.7 | 140.876 | 4.97 |
| 0.8006 | 222.9 | 1049.3 | 1587.0 | −0.529 | 3.784 | 26.008 | −0.241 | 44.8 | 141.898 | 5.35 |
| 1.0000 | | 1046.5 | 1543.7 | 0.000 | 4.010 | 31.362 | 0.000 | 0.0 | | |
| | | | | | | *333.15* | | | | |
| 0.0000 | 0.00 | 983.2 | 1551.0 | 0.000 | 4.228 | 4.001 | 0.000 | 0.0 | | |
| 0.0200 | 1.13 | 993.0 | 1644.1 | −0.033 | 3.725 | 4.621 | −0.506 | 100.2 | 141.336 | 0.74 |
| 0.0501 | 2.93 | 1019.4 | 1712.2 | −0.451 | 3.346 | 5.445 | −0.884 | 175.2 | 134.019 | 1.42 |
| 0.1001 | 6.17 | 1036.9 | 1750.3 | −0.767 | 3.148 | 6.840 | −1.073 | 219.5 | 135.336 | 2.48 |
| 0.1010 | 6.23 | 1035.0 | 1740.3 | −0.708 | 3.190 | 6.866 | −1.030 | 209.6 | 135.984 | 2.65 |
| 0.2006 | 13.9 | 1051.5 | 1723.5 | −1.177 | 3.202 | 9.578 | −0.996 | 197.5 | 137.130 | 3.64 |
| 0.3010 | 23.9 | 1051.0 | 1690.4 | −1.142 | 3.330 | 12.360 | −0.848 | 165.6 | 139.210 | 4.25 |
| 0.3978 | 36.7 | 1052.6 | 1653.9 | −1.233 | 3.473 | 14.975 | −0.689 | 129.1 | 139.909 | 4.65 |
| 0.4976 | 55.0 | 1050.5 | 1619.5 | −1.081 | 3.630 | 17.692 | −0.520 | 94.5 | 140.835 | 5.00 |
| 0.5972 | 82.3 | 1050.0 | 1612.2 | −1.018 | 3.664 | 20.449 | −0.474 | 86.8 | 141.301 | 5.11 |
| 0.8006 | 222.9 | 1046.1 | 1570.7 | −0.535 | 3.875 | 26.000 | −0.248 | 44.4 | 142.337 | 5.50 |
| 1.0000 | | 1043.2 | 1527.0 | 0.000 | 4.111 | 31.349 | 0.000 | 0.0 | | |

$u(p) < \pm 0.39$ kPa.
[a] Standard uncertainties are: $u(x_{IL}) = \pm 10^{-4}$.
[b] Standard uncertainties are: $u(m) = \pm 0.002$ mol · kg$^{-1}$.
[c] Standard uncertainties are: $u(\rho) = \pm 0.86$ kg · m$^{-3}$.
[d] Standard uncertainties are: $u(u) = \pm 1.2$ m · s$^{-1}$.
[e] Standard uncertainties are: $u(V_m^E) = \pm 0.10$ · cm$^3$ · mol$^{-1}$ (max).
[f] Standard uncertainties are: $u(k_S) = \pm 6.0 \cdot 10^{-13}$ · Pa$^{-1}$ (max).
[g] Standard uncertainties are: $u(k_m) = \pm 7.0 \cdot 10^{-7}$ m$^3$ · mol$^{-1}$ · Pa$^{1/7}$ (max).
[h] Standard uncertainties are: $u(V_\phi) = \pm 0.57$ cm$^3$ · mol$^{-1}$ (max).
[i] Standard uncertainties are: $u(k_\phi) = \pm 5.4 \cdot 10^{-16}$ m$^3$ · mol$^{-1}$ · Pa$^{-1}$ (max).

**TABLE 4**
Fitting parameters of equations (6) and (7) with 95% of confidence limits, and standard deviations for the system {m2HEAPr(1) + $H_2O$(2)}.

| Equation (6) | | | | | | | | |
|---|---|---|---|---|---|---|---|---|
| $C_0$ | $C_1$ | $C_2$ | | | | | | |
| 43.6838 | −66.7521 | 95.7529 | | | | $\sigma_\rho = 4.5$ kg · m$^{-3}$ | *AAD* = 0.38%[a] | |
| | | | | *Equations (7)–(9)* | | | | |
| | $C_{0j}$ | $C_{1j}$ | $C_{2j}$ | $D_{1j}$ | $D_{2j}$ | $D_{3j}$ | | |
| j = 0 | $-8.98322 \cdot 10^6$ | $1.60533 \cdot 10^7$ | $-1.08452 \cdot 10^7$ | $-1.4581 \cdot 10^8$ | $-8.95004 \cdot 10^7$ | 0 | $\sigma_\rho = 1.9$ kg · m$^{-3}$ | *AAD*=0.13%[a] |
| j = 1 | $3.71686 \cdot 10^4$ | $-6.22854 \cdot 10^4$ | $3.84328 \cdot 10^4$ | $5.78039 \cdot 10^5$ | $3.74511 \cdot 10^5$ | 0 | | |
| j = 0 | 0.585137 | 0.62323 | −0.154036 | 2.35614 | 1.6716 | 0.388938 | $\sigma_\rho = 0.6$ kg · m$^{-3}$ | *AAD* = 0.04%[a] |
| j = 1 | −0.00240257 | −0.00143076 | $2.06855 \cdot 10^{-3}$ | $2.59148 \cdot 10^{-3}$ | $4.86712 \cdot 10^{-3}$ | $1.89321 \times 10^{-3}$ | | |
| j = 2 | $3.2547 \cdot 10^{-6}$ | $1.66029 \cdot 10^{-6}$ | $-3.15268 \cdot 10^{-6}$ | $2.0159 \cdot 10^{-7}$ | $1.75973 \cdot 10^{-6}$ | $2.06578 \times 10^{-6}$ | | |

[a] Average absolute deviation, $\mathrm{AAD}\% = (100/N_p)\sum_{i=1}^{N_p}|(\rho_{calc} - \rho)/\rho|_i$ where $\rho_{calc}$ and $\rho$ are the calculated and experimental values of density.

(9) are presented in table 4. The correlation of density with equations (7)–(9) is good over the whole temperature and composition ranges with a standard deviation of 1.9 kg · m$^{-3}$, and *AAD* = 0.13%. The relative deviations between the calculated density values (by equation (7)) and the experimental ones are presented in figure 1. Deviations are more significant only at the mole fraction of ionic liquid $x_1 = 0.02$ and for temperatures higher than 308.15 K. The deviations between calculated and experimental values are usually much lower than for the Jouyban–Acree model for all compositions and temperatures. When more coefficients are added in the Padé

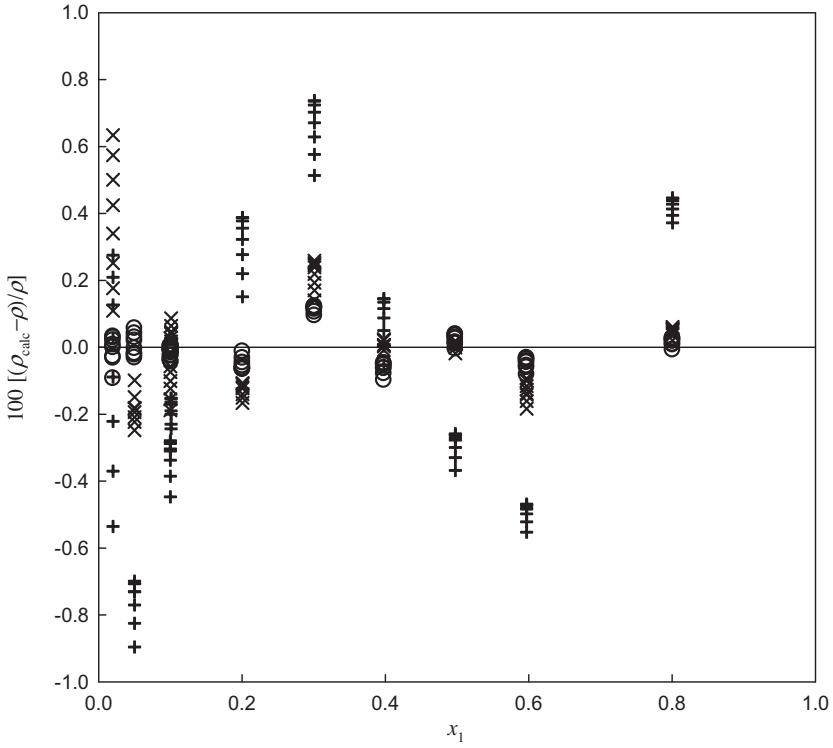


**FIGURE 1.** Relative deviations between the calculated density values with correlation equations, $\rho_{calc}$, and the experimental values, $\rho$, for the mixtures {m2HEAPr(1) + $H_2O$(2)} as a function of $x_1$ and temperature: +, Jouyban-Acree model, equation (6); ×, ○, Padé approximant, equation (7) with 10 and 18 coefficients, respectively.

approximant the deviations become lower. In figure 1 the deviations obtained with equation (7) fitted with 18 coefficients given in table 4 using quadratic dependencies in the temperature for $C_i$ and $D_i$ are also displayed. For this situation the deviations are very small (corresponding to a standard deviation of 0.6 kg · m$^{-3}$, and *AAD* = 0.04%). It must be referred that some authors use high number of correlating coefficients in density equations for the same kind of systems of the studied in this work. Alvarez *et al.* [59] report 18 coefficients for ethylammonium acetate (+water, methanol, or ethanol) with standard deviations ranging from (0.4 to 1.8) kg · m$^{-3}$.

The molar volume $V_m$, was determined from density values using equation (1) where $\rho$ is the mixture density and $M = (x_1M_1 + x_2M_2)$ is the corresponding molar mass. For the binary systems, the excess molar volumes $V_m^E$ were calculated using the experimental mixture and the pure components densities as described by equation (10):

$$V_m^E = \frac{M}{\rho} - \frac{x_1M_1}{\rho_1} - \frac{x_2M_2}{\rho_2}. \quad (10)$$

Data for this property are presented in table 3. The uncertainty in $V_m^E$, $u(V_m^E)$, estimated using the errors propagation method was ±0.03 cm$^3$ · mol$^{-1}$ and ±0.10 cm$^3$ · mol$^{-1}$ at the lower and upper limits of ionic liquid concentrations, respectively by using the experimental density and mole fraction uncertainties. The binary $V_m^E$ experimental values were fitted by means of rational functions [73] (equation (11)):

$$V_m^E/(\mathrm{Pa}^{-1}) = x_1x_2\frac{\sum_{i=0}^{m}A_i(2x_1-1)^i}{1+\sum_{i=1}^{n}B_i(2x_1-1)^i}, \quad (11)$$

where $A_i$ and $B_i$ are the adjustable coefficients given by quadratic equations on temperature:

$$A_i = A_{i,0} + A_{i,1}T + A_{i,2}T^2, \quad (12)$$

$$B_i = B_{i,0} + B_{i,1}T + B_{i,2}T^2. \quad (13)$$

The coefficients $A_{ij}$ and $B_{ij}$ (j = 0,2) of equations (12) and (13) are given in table 5 together with the standard deviation $\sigma(V_m^E)$. The experimental values of the excess molar volumes for the binary system m2HEAPr(1) + $H_2O$(2) are plotted in figure 2. The values of $V_m^E$ are negative for all the temperatures over the whole composition range and its temperature dependency is minimal for fixed compositions. The values in the ionic liquid mole fraction range between 0.2 and 0.6 are significantly high (−1cm$^3$ · mol$^{-1}$). In figure 2 the $V_m^E$ values for the aqueous mixtures of 2-hydroxyethylammonium acetate (2HEAAc) [59] at $T$ = (293.15 and 323.15) K are also plotted. For this range of temperatures, the changes in $V_m^E$ are also minimal. The absence of the methyl group in the ammonium (2HEA) ion and the inclusion of the acetate anion (Ac), shift $V_m^E$ for less negative values compared with those obtained for m2HEAPr. The $V_m^E$ curves from equation (11) are also represented in figure 2. They are asymmetric with a minimum at mole fraction of ionic liquid between 0.3 and 0.4. The significant size and negative sign of $V_m^E$ values reflect the type of interactions taking place in the mixtures, which are the result of different effects, namely the breakdown of the self-associated water molecules (positive contribution to volume), the packing effect, and the (ion + dipole) interaction of water molecules with ionic liquid (negative contributions to the volume). The mole fraction range $x_1$ = (0.3 to 0.4) corresponds probably to the highest packing between water and the ionic liquid. The molar volumes of the pure m2HEAPr are between 140 cm$^3$ · mol$^{-1}$ at $T$ = 298.15 K and 143 cm$^3$ · mol$^{-1}$ at $T$ = 333.15 K, being much greater than the molar volume of water (18.02 cm$^3$ · mol$^{-1}$). These large differences

**TABLE 5**
Fitting parameters of rational functions (11) used for analytical representation of $V_m^E$, $k_S^E$, and $u^E$, with 95% of confidence limits, and standard deviations for the system {m2HEAPr(1) + $H_2O$(2)}.

| | $A_{0j}$ | $A_{1j}$ | $A_{2j}$ | $A_{3j}$ | $A_{4j}$ | $B_{1j}$ | $B_{2j}$ | |
|---|---|---|---|---|---|---|---|---|
| $V_m^E/(cm^3 \cdot mol^{-1})$ | | | | | | | | |
| j = 0 | −28.2381 | −78.1075 | −51.3634 | 0 | 0 | 8.5594 | 7.8238 | $\sigma(V_m^E) = 0.044$ |
| j = 1 | 0.1534 | 0.461995 | 0.3182 | 0 | 0 | $-4.2174 \cdot 10^{-2}$ | $-4.3881 \cdot 10^{-2}$ | |
| j = 2 | $-2.4623 \cdot 10^{-4}$ | $-7.3008 \cdot 10^{-4}$ | $-4.9784 \cdot 10^{-4}$ | 0 | 0 | $6.4847 \cdot 10^{-5}$ | $6.7489 \cdot 10^{-5}$ | |
| $10^{10} k_S^E/Pa^{-1}$ | | | | | | | | |
| j = 0 | −10.3733 | 15.5340 | 41.5112 | 0 | 0 | 4.5362 | −0.3809 | $\sigma(k_S^E) = 0.016$ |
| j = 1 | $5.3540 \cdot 10^{-2}$ | $-9.4488 \cdot 10^{-2}$ | −0.28121 | 0 | 0 | $-2.0353 \cdot 10^{-2}$ | $4.5134 \cdot 10^{-3}$ | |
| j = 2 | $-8.7076 \cdot 10^{-5}$ | $1.4458 \cdot 10^{-4}$ | $4.5893 \cdot 10^{-4}$ | 0 | 0 | $2.9325 \cdot 10^{-5}$ | $-9.1201 \cdot 10^{-6}$ | |
| $u^E/(m \cdot s^{-1})$ | | | | | | | | |
| j = 0 | 2554.53 | −1125.66 | 1587.09 | 3006.08 | −21243.5 | 9.2149 | 0 | $\sigma(u^E) = 3.8$ |
| j = 1 | −11.1005 | 5.4384 | −0.4489 | −26.4441 | 129.671 | $-5.4148 \cdot 10^{-2}$ | 0 | |
| j = 2 | $1.3926 \cdot 10^{-2}$ | $-6.8479 \cdot 10^{-3}$ | $-9.4869 \cdot 10^{-3}$ | $5.0927 \cdot 10^{-2}$ | −0.200073 | $8.7532 \cdot 10^{-5}$ | 0 | |

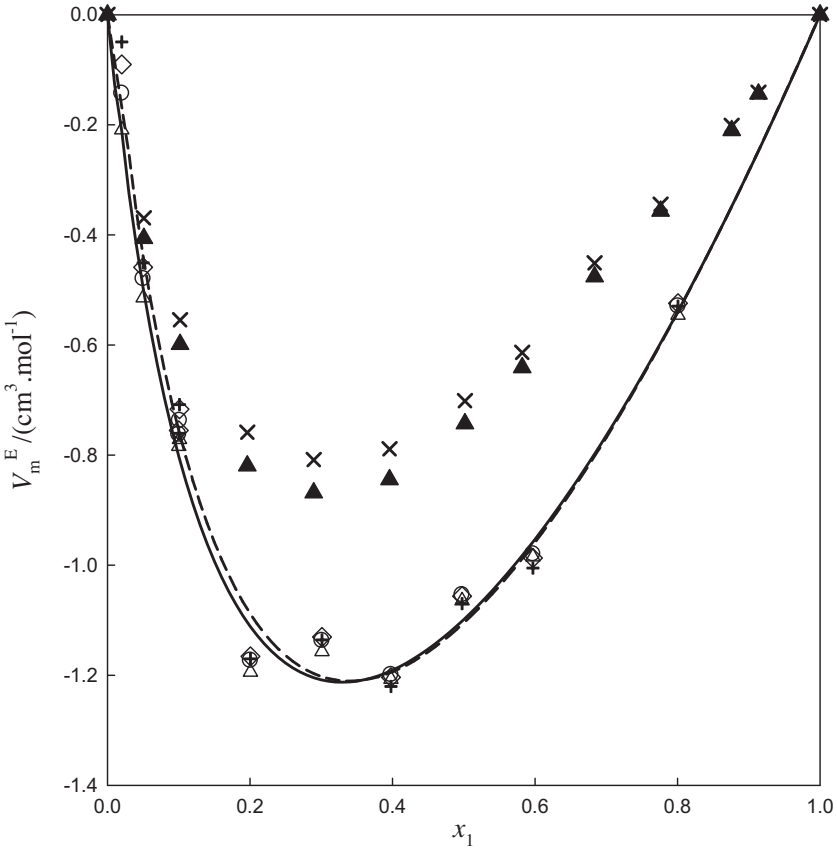


**FIGURE 2.** Excess molar volumes, $V_m^E$, as a function of m2HEAPr mole fraction, $x_1$ at several temperatures. For {m2HEAPr(1) + $H_2O$(2)}: △, $T$ = 298.15 K; ○, $T$ = 308.15 K; □, $T$ = 318.15 K; +, $T$ = 328.15 K. Solid and dashed curves were calculated from equation (11) at $T$ = 298.15 K and $T$ = 328.15 K, respectively. For {2HEAA(1) + $H_2O$(2)} [59]: ▲, $T$ = 288.15 K; ×, $T$ = 323.15 K.

between molar volumes have as a consequence that the small water molecules fit the available space or free volume of the ionic liquid upon mixing.

The apparent molar volumes, $V_\phi$, of m2HEAPr in the aqueous mixtures were calculated using equation (14):

$$V\phi = \frac{M_1}{\rho} + \frac{(\rho_2 - \rho)}{m\rho_2\rho}, \tag{14}$$

where $m$ (mol · $kg^{-1}$) is the molality of m2HEAPr in water. From the error in mole fraction, the maximum uncertainty in molality, $u(m)$, was ±0.002 mol · $kg^{-1}$. The uncertainty in $V_\phi$, $u(V_\phi)$, was obtained from the errors propagation method. Uncertainties of the order of ±0.57 $cm^3 \cdot mol^{-1}$ were found at low ionic liquid content decreasing to ±0.11 $cm^3 \cdot mol^{-1}$ at high concentrations. The calculated apparent molar volumes are given in table 3 and plotted in figure 3 as function of the IL molality. The apparent molar volume increases rapidly at low concentrations (up to $m \approx 25$ kg · $mol^{-1}$) and then it is almost constant.

To describe the molality dependence of apparent molar volumes, the empirical Redlich–Rosenfeld–Meyer equation [74] and the Pitzer equation [75], both derived from the Debye–Hückel limiting law (DHLL), have been used. The Redlich–Rosenfeld–Meyer

and Pitzer equations can be given by equations (15) and (16), respectively:

$$V_\phi = V_\phi^0 + A_V(m)^{1/2} + B_V m \tag{15}$$

and

$$V_\phi = V_\phi^0 + A_V b^{-1} \ln\left(1 + b(m)^{1/2}\right) + B'_V m \tag{16}$$

where $A_V$ is the Debye–Hückel limiting slope, reflecting the volumetric and dielectric properties of water, the slopes $B_V$ and $B'_V$ are empirical constants obtained by fitting to the molar apparent volumes, and the parameter $b$ has a universal value of 1.2 $kg^{1/2} \cdot mol^{-1/2}$ [17,75]. The theoretical expression of $A_V$ is well known [75,76] and the equivalence of the limiting slope in equations (15) and (16) was demonstrated by Ananthaswamy and Atkinson [77]. The limiting apparent molar volume,$V_\phi^0$, $(V_\phi(m \to 0))$, gives the extent of (ion + solvent) interactions [78] as it depends on the solvent relative permittivity, size and charge of the ions, pressure and temperature. The $B_v$ slopes are related with deviations from DHLL, which can be understood in terms of interactions between ion solvation shells, depending on temperature, solvent, and the electrolyte [79–81]. In solvents of low electric permittivity, experimentally determined $B_v$ values include contributions from the formation of ion pairs [82]. This can be the case of alcohols for which the relative permittivities, $\varepsilon_r$, are low (at $T$ = 298.15 K: methanol, $\varepsilon_r$ = 32.66 [83]; ethanol, $\varepsilon_r$ = 24.35 [84]) compared to water ($\varepsilon_r$ = 78.36 at $T$ = 298.15 K [83]). Apparent molar volumes at infinite dilution, $V_\phi^0$ , of m2HEAPr in water were determined using least-squares fittings to the linear plots of $V_\phi{}^1 = V_\phi - A_V(m)^{1/2}$ or $V_\phi{}^2 = V_\phi - A_V b^{-1} \ln\left(1 + b(m)^{1/2}\right)$ versus molality using the apparent molar volume values given in table 3 within the range ($m$ < 25 mol · $kg^{-1}$), where $V_\phi^1$ and $V_\phi^2$ follow almost a linear behaviour on molality, verified in dilute electrolyte solutions. The $A_V$ values used at the different temperatures are those recommended by Archer and Wang [85]. They are given in table 6 as well as the $V_\phi^0$ , and the slopes $B_V$ and $B'_V$ of equations (15) and (16). It can be concluded that the $V_\phi^0$ values are all large and positive, which is due to the strong (ion + solvent) interactions at infinite dilution ((ion + ion) interactions vanish at infinite dilution).

The apparent molar volumes as function of IL molality and temperature for the whole concentration and temperature ranges were described by the function showed by equation (17):

$$V\phi = V_\phi^0(T) + \frac{A(T)(m)^{1/2} + B(T)m}{1 + C(T)m}, \tag{17}$$

where $V_\phi^0(T)$, $A(T)$, $B(T)$, and $C(T)$ are linear functions of temperature: $V_\phi^0 = v_1 + v_2T$, $A(T) = a_1 + a_2T$, $B(T) = b_1 + b_2T$, $C(T) = c_1 + c_2T$.

For dilute solution of IL $(m \to 0)$ equation (17) gives equation (15). The parameters $v$, $a$, $b$ and $c$ of equation (17) are

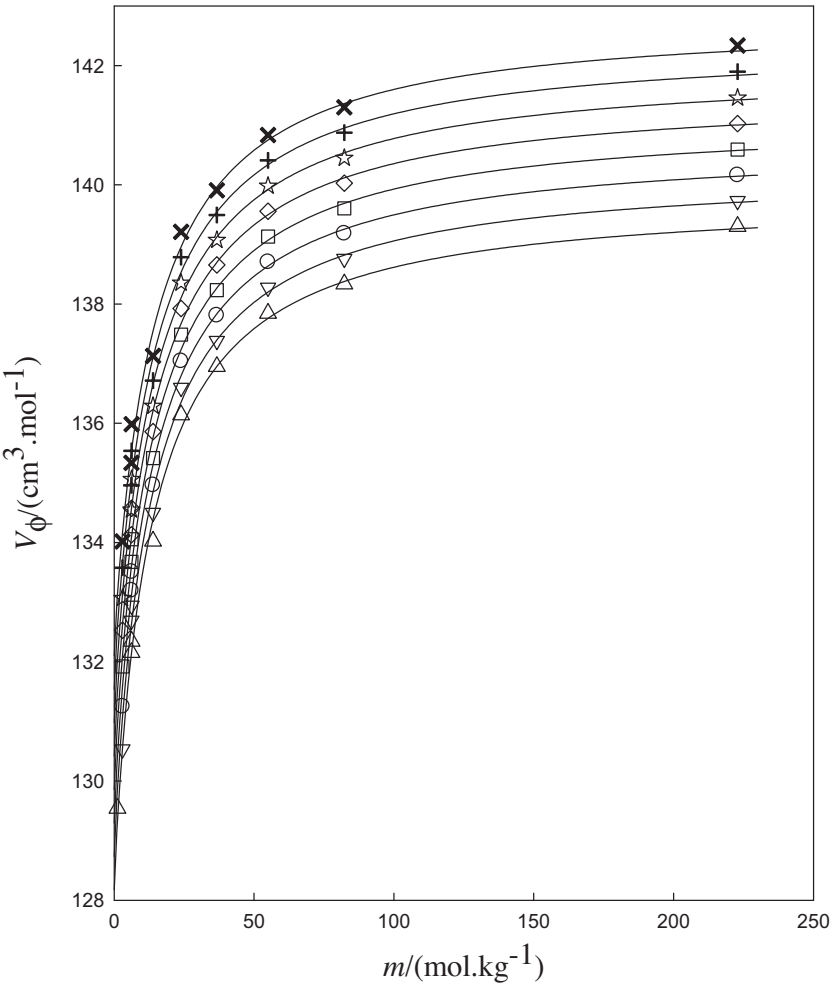


**FIGURE 3.** Apparent molar volume, $V\phi$, versus molality, $m$, at several temperatures for {m2HEAPr(1) + $H_2O$(2)}: △, $T$ = 298.15 K; ▽, $T$ = 303.15 K; ○, $T$ = 308.15 K; □, $T$ = 313.15 K; ◇, $T$ = 318.15 K; ;☆, $T$ = 323.15 K ; +, $T$ = 328.15 K, ×, $T$ = 333.15 K. Solid curves were calculated from equation (17).

**TABLE 6**
Theoretical Debye–Hückel limiting slope $A_V$ for a 1:1 electrolyte in water, infinite dilution partial molar volume $V_\phi^0$ and empirical parameters $B_V$ and $B'_V$ for m2HEAPr in water at several temperatures.

| $T$/K | [a]$A_V$/cm$^3$ · kg$^{1/2}$ · mol$^{-3/2}$ | $V_\phi^0$ equation (15)/ cm$^3$ · mol$^{-1}$ | $V_\phi^0$ equation (16)/ cm$^3$ · mol$^{-1}$ | $V_\phi^0$ equation (17)/ cm$^3$ · mol$^{-1}$ | $B_V$/cm$^3$ · kg · mol$^{-2}$ | $B'_V$ /cm$^3$ · kg · mol$^{-2}$ | $\sigma$ equation (15) | $\sigma$ equation (16) |
|---|---|---|---|---|---|---|---|---|
| 298.15 | 1.8305 | 127.73 | 128.22 | 128.18 | −0.0244 | 0.2198 | 0.2 | 0.6 |
| 303.15 | 1.9214 | 128.26 | 129.36 | 128.74 | −0.0489 | 0.1730 | 0.2 | 0.7 |
| 308.15 | 2.0198 | 128.33 | 130.41 | 129.30 | −0.0496 | 0.1305 | 0.4 | 1.1 |
| 313.15 | 2.1256 | 128.57 | 129.99 | 129.90 | −0.0644 | 0.1747 | 0.2 | 0.5 |
| 318.15 | 2.2389 | 128.96 | 130.44 | 130.42 | −0.0872 | 0.1654 | 0.2 | 0.4 |
| 323.15 | 2.3601 | 129.28 | 130.83 | 130.98 | −0.1086 | 0.1581 | 0.2 | 0.4 |
| 328.15 | 2.4894 | 129.56 | 131.19 | 131.54 | −0.1300 | 0.1516 | 0.3 | 0.4 |
| 333.15 | 2.6273 | 129.77 | 131.48 | 132.10 | −0.1502 | 0.1473 | 0.3 | 0.4 |

[a] The values of $A_V$ in reference [85] were expressed in terms of cm$^3$ · kg$^{1/2}$ · mol$^{-3/2}$.

$v_1 = 94.75$ cm$^3$ · mol$^{-1}$, $v_2 = 0.1121$ cm$^3$ · mol$^{-1}$ · K$^{-1}$, $a_1 = -0.2058$ cm$^3$ · mol$^{-3/2}$ · kg$^{-1/2}$, $a_2 = 1.6610 \cdot 10^{-3}$ cm$^3$ · mol$^{-3/2}$ · kg$^{-1/2}$ · K$^{-1}$, $b_1 = 2.3614$ cm$^3$ · mol$^{-2}$ · kg, $b_2 = -5.2262 \cdot 10^{-3}$ cm$^3$ · mol$^{-2}$ · kg · K$^{-1}$, $c_1 = 0.161312$ kg · mol$^{-1}$, and $c_2 = -3.0723 \cdot 10^{-4}$ kg · mol$^{-1}$ · K$^{-1}$. The correlation of apparent molar volume with equation (17) is excellent with a standard deviation of 0.2 cm$^3$ · mol$^{-1}$, an *AAD* = 0.04%, and a maximum deviation of 0.12%. The limiting values $V_\phi^0$ from equation (17) are compared with those obtained from equations (15) and (16) in table 6. The limiting apparent molar volume values obtained from data fitting by equation (15) are lower than those resulting from equations (16) and (17), however the computed values from the two later equations are in good agreement. The limiting apparent molar volume expansibility, $\alpha_p^0 = (\partial V_\phi^0/\partial T)_p$ , is positive ($\alpha_p^0 \approx 0.112$ cm$^3$ · mol$^{-1}$ · K$^{-1}$). This means that on heating some water molecules can be released from the hydration layers [14]. Higher positive values of $\alpha_p^0$ have been observed for aqueous imidazolium-based ILs [14] whereas negative values are observed for alcoholic mixtures of ILs [14].

### 3.3. Acoustical properties

The speed of sound measurements for pure methyl-2-hydroxyethylammonium propionate at atmospheric pressure and temperature range $T = (293.15$ to $343.15)$ K are presented in table 2 and plotted in figure 4. The values reported by Álvarez *et al.* [69] are also represented. The measured values presented by those authors are always significantly higher than the ones from this study with deviations from (3 to 4)% at $T = (293.15$ and $338.15)$ K, respectively.

The speed of sound values have been correlated with temperature using the equation (18):

$$u = u_0 (1 - T/T_c)^m, \tag{18}$$

where $u_0$ is the speed of sound at absolute zero, $T_c$ is the critical temperature, $m$ and $u_0$ are fitting parameters. Rao proposed equation (18) with $m = 0.9$ [86]. It is interesting to note that the equation (16) shows a temperature dependency similar to that proposed by Guggenheim [87]. The critical temperature for ionic liquids can be obtained by a group contribution method proposed by Valderrama *et al.* [88] (equation (19)):

$$T_c = T_b \left[ 0.5703 + 1.0121 \sum_k n_k \Delta_{T_{c,k}} - \left( \sum_k n_k \Delta_{T_{c,k}} \right)^2 \right]^{-1}, \tag{19}$$

where $n_k$ and $\Delta_{T_{c,k}}$, are the occurrences number of group k in the ion, and the contribution for group k, respectively, and $T_b$ is the normal boiling point calculated with equation (20):

$$T_b = 198.2 + \sum_k n_k \Delta_{T_{b,k}}, \tag{20}$$

where $\Delta_{T_{b,k}}$ is contribution for group k. For m2HEAPr, the calculations give $T_c = 738.08$ K. The fitting by least squares of equation (18) to the speed of sound data of this work led to $u_0 = (2573.1 \pm 11.3)$ m · s$^{-1}$ and $m = (0.8710 \pm 0.0078)$, with standard deviation $\sigma_u = 1.5$ m · s$^{-1}$.

Recently, Wu *et al.* [89] proposed a corresponding states group contribution method for estimating the speed of sound of ILs based on the speed of sound database of pure ILs created by collecting experimental data from literature between 2005 and 2013. The proposed equation by the method is showed in equation (21):

$$u = \sum_{i=0}^{3} a_i \left( \sum_{j=1}^{k} n_j \Delta u_{0j} \right)^i (1 - T/T_c)^{0.65359}, \tag{21}$$

where $n_j$ is the number of groups of type j, k is the total number of different groups in the ionic fragment, and $a_i$ and $\Delta u_{0,j}$ are parameters and group contribution parameter for group j, respectively, which were given by authors [89]. An average absolute deviation (*AAD*) of 2.34% has been obtained for a total of 96 ionic liquids covering imidazolium, pyridinium, pyrrolidinium, phosphonium, and ammonium cations combined with a large variety of anions. In figure 4, the speed of sound values, calculated from equation (21), are compared to those from this study. The predicted values from the Wu *et al.* equation are in good agreement with the measured values in this study with a maximum deviation of +2% at $T = 343.15$ K.

Measurements of the speed of sound in aqueous electrolyte solutions provide information about ion-ion and (ion + solvent) interactions [90]. Based on the measured speed of sound and density values reported in table 3, the isentropic compressibility of the mixture, $k_S$, was calculated from the Laplace–Newtońs equation $k_s = (1/\rho u^2)$. The uncertainty in $k_S$, $u(k_S)$, was obtained using the standard deviations for the experimental density and speed of sound in the errors propagation method. Maximum uncertainty of the order $\pm 6.0 \cdot 10^{-13}$ Pa$^{-1}$ was found. The excess isentropic compressibility $k_S^E = k_S - k_S^{id}$ , was calculated using the rigorous thermodynamic ideal-mixing rule for isentropic compressibility $k_S^{id}$ . Douhéret *et al.* [91] stated that this ideal-mixing rule can be correctly obtained from the expression found by Benson and Kiyohara for the ideal mixture [92] (equation (22)):

$$k_S^{id} = \sum_{i=1}^{2} \phi_i k_{S,i} + T \left[ \sum_{i=1}^{2} \frac{\phi_i V_{m,i} \alpha_{p,i}^2}{C_{p,m,i}} - \frac{V_m^{id} (\alpha_p^{id})^2}{C_{p,m,i}^{id}} \right]. \tag{22}$$

In equation (22), $\phi_i (= x_i V_{m,i}/V_m^{id})$ is the volume fraction of the i component in the mixture, whereas $\alpha_{p,i}$ and $C_{p,m,i}$ are the thermal expansivity and molar heat capacity, respectively, of pure i component. The $V_m^{id}$ $\left(= \sum_i^2 x_i V_{m,i}\right)$, $\alpha_p^{id}$ $\left(= \sum_i^2 \phi_i \alpha_{p,i}\right)$ and $C_{p,m}^{id}$ $\left(= \sum_i^2 x_i C_{p,i}\right)$

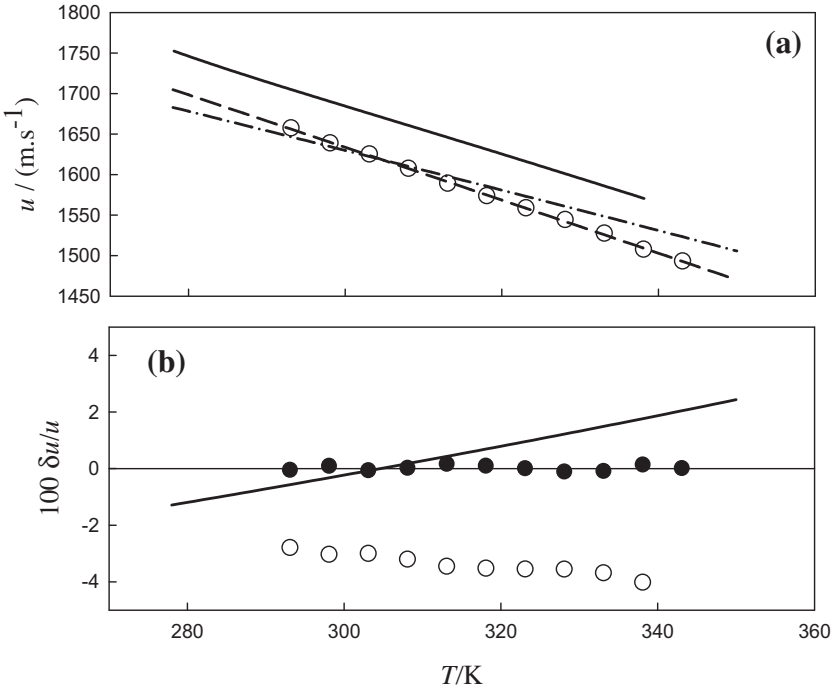


**FIGURE 4.** (a) Speed of sound, $u$, of m2HEAPr as a function of temperature: ○, Experimental values are from this work; solid line, Álvarez *et al.* [69]; ----, correlation with equation (18); –·–, prediction with Wu *et al.* [89] method. (b) relative deviations of: ○, experimental values from this work from values measured by Álvarez *et al.*; ●, experimental values from this work from equation (18); solid line, equation (18) from Wu *et al.* method.

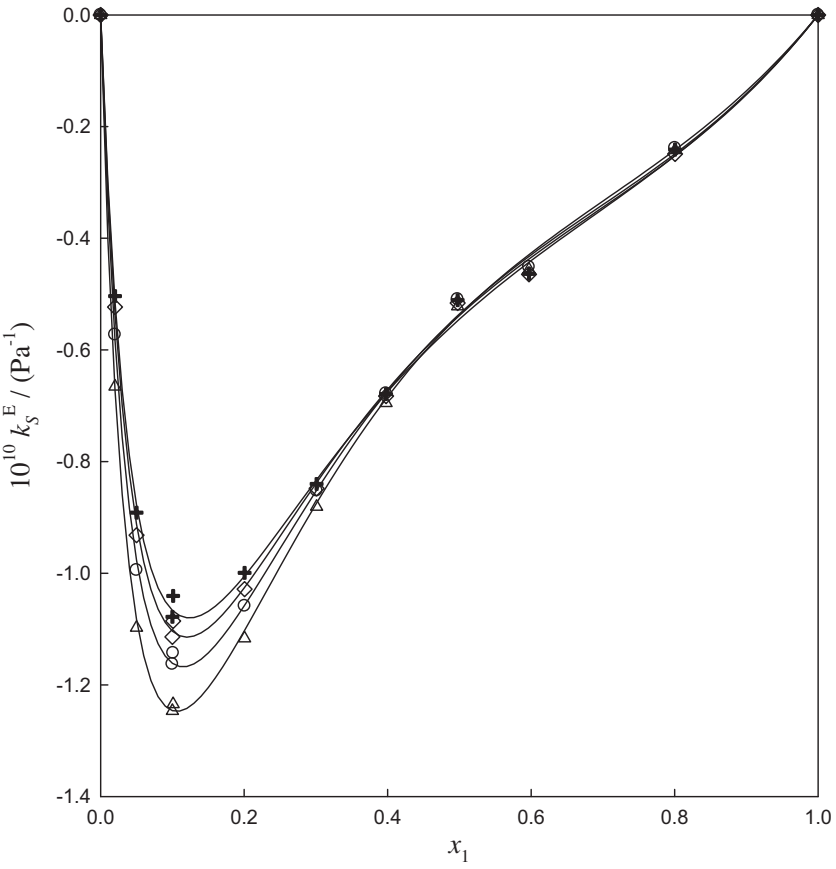


**FIGURE 5.** Excess isentropic compressibility, $k_S^E$ , of {m2HEAPr(1) + $H_2O$(2)} liquid mixtures as a function of mole fraction, $x_1$, at several temperatures. △, $T$ = 298.15 K; ○, $T$ = 308.15 K; ◇, $T$ = 318.15 K; +, $T$ = 328.15 K. Solid curves were calculated from equation (11).

are the molar volume, thermal expansivity and molar isobaric heat capacity, respectively, of the ideal mixture. The $k_S^E$ values were correlated with the IL mole fraction $x_1$, by the rational functions (11). The correlation coefficients are given in table 5 with the standard deviations $\sigma(k_S)$ . In figure 5, the $k_S^E$ values and the curves obtained from the rational functions are presented for the binary system (m2HEAPr(1) + $H_2O$(2)). The excess isentropic compressibility is always negative for the whole range of temperatures and compositions and becomes less negative when temperature increases. The $k_S^E$ curves are remarkably asymmetric, with sharp minima at low values of IL mole fraction ($x_1 \approx 0.12$). The high negative values of the (IL + water) mixtures are due to the closer proximity between water molecules and IL ions, and the strong interaction between them, leading to a compressibility decreasing.

Douhéret *et al.* [91] also stated that the speed of sound in an ideal-mixture may be calculated as with equation (23)

$$u^{id} = (\rho^{id} k_S^{id})^{-1/2} = \left(\frac{V_m^{id}}{k_S^{id} M}\right)^{1/2}. \quad (23)$$

From equation (23) the excess speed $u^E$ ($=u - u^{id}$) can be calculated. The values are included in table 3 and they were correlated using the rational functions (11) whose coefficients and standard deviation $\sigma(u^E)$ are given in table 5. The excess speed of sound is plotted in figure 6. It is observed that $u^E$ is always positive over the whole range of temperatures and compositions, but it decreases when the temperature increases. The fitted curves are very asymmetric as well, presenting a maximum at the low IL mole fraction ($x_1 \approx 0.12$) as well as for $k_S^E$. The excess isentropic compressibility and the excess speed of sound are closely related as follows. Taking into account that $k_S^E = k_S - k_S^{id}$, that $k_s = (1/\rho u^2)$, and that $u^E = u - u^{id}$ where $u^{id}$ is given by equation (23) one obtains

$$u^E = \frac{1}{\rho^{1/2}(k_S^E + k_S^{id})^{1/2}} - \frac{1}{\rho_{id}^{1/2}(k_S^{id})^{1/2}}. \quad (24)$$

Therefore, the excess speed of sound is closely related with $k_S^E$ . Furthermore, subtraction of term $1/\rho_{id}^{1/2}(k_S^{id})^{1/2}$ to $1/\rho^{1/2}(k_S^E + k_S^{id})^{1/2}$ will withdraw influence of $k_S^{id}$ and then evidencing more the analytical influence of $k_S^E$ in $u^E$. The almost symmetrical shape between figures 5 and 6 can be explained in this way.

It is possible that at 0.10 and 0.50–0.60 IL mole fractions the level of uncertainty in the speed of sound measurement may be about two times the expanded uncertainty ($U(u) = \pm 2.4\ m \cdot s^{-1}$ for confidence level 95% (coverage factor k = 2)) and lower than the expanded uncertainty value at the remaining compositions. This possibility is grounded in the calculation of the absolute speed of sound deviations between experimental and calculated values from the excess speed of sound described analytically by the equation similar to equation (11) for the studied mole fractions and temperatures. The higher uncertainties are probably due to several factors such as the error in the mole fraction determination possibly higher at the before mentioned points and to the abrupt change in speed of sound near $x_{IL} = 0.10$ (see table 3) where small deviations in mole fraction could increase the uncertainty. However the analysis of the uncertainty presented before should be taken with some caution because it depends also on the non-ideality of the mixture and the {m2HEAPr(1) + water(2)} is a strong non-ideal

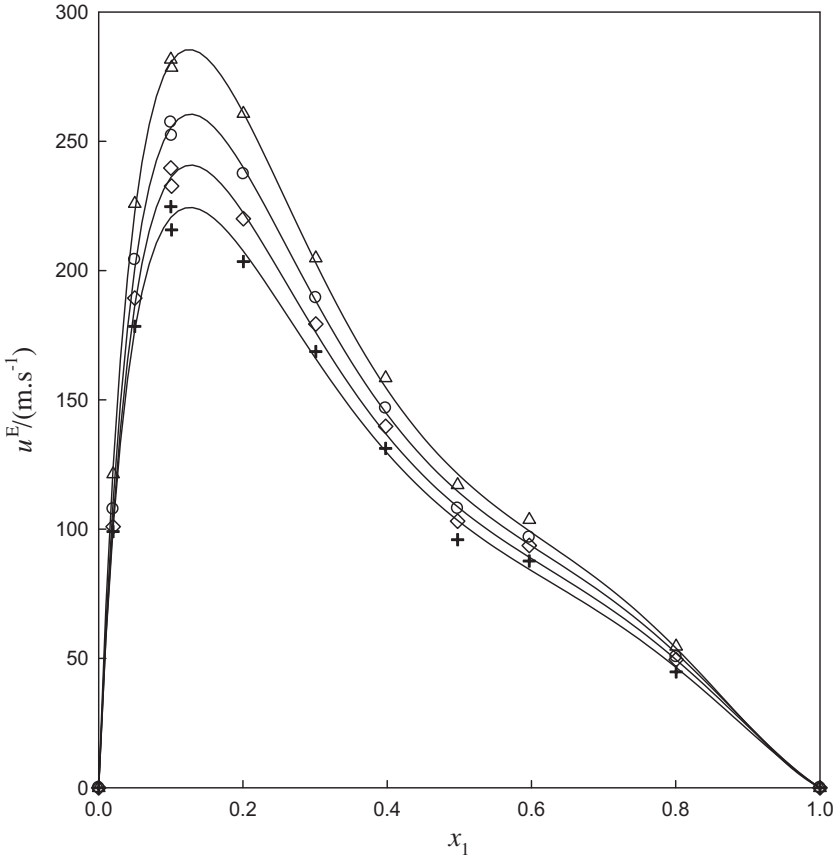


**FIGURE 6.** Excess speed of sound, $u^E$, of {m2HEAPr(1) + $H_2O$(2)} liquid mixtures as a function of mole fraction, $x_1$ at several temperatures. △, $T = 298.15$ K; ○, $T = 308.15$ K; ◇, $T = 318.15$ K; +, $T = 328.15$ K. Solid curves were calculated from equation (11).

system as can be seen by excess molar volume and excess speed of sound.

The apparent IL molar isentropic compressibility values, $k_\phi$, in the aqueous mixtures were computed using equation (25):

$$k_\phi = \frac{k_S M_1}{\rho} + \frac{(k_S\rho_2 - k_{S,2}\rho)}{m\rho_2\rho}, \quad (25)$$

where $k_{S,2}$ and $k_s$ represent the isentropic compressibility of the water and the binary mixture (IL+water), respectively. Uncertainties in $k_\phi$, $u(k_\phi)$, of the order of $\pm 5.4 \cdot 10^{-16}$ m$^3 \cdot$ mol$^{-1} \cdot$ Pa$^{-1}$ and $\pm 1.0 \cdot 10^{-16}$ m$^3 \cdot$ mol$^{-1} \cdot$ Pa$^{-1}$ were estimated at low and high concentrations of ionic liquid, respectively. Values of the calculated apparent molar compressibility from equation (23) are given in table 3 and plotted in figure 7 as function of the IL molality and temperature. The apparent molar compressibility increases rapidly up to $m \approx 25$ kg $\cdot$ mol$^{-1}$ and then is almost constant with molality. The same behaviour was also verified for the apparent molar volume.

Equation (26)

$$k_\phi = k_\phi^0 + A_k(m)^{1/2} + B_k m \quad (26)$$

proposed by Dey *et al.* [93], was used to describe the molality dependence of $k_\phi$, where $A_k$ is the Debye-Hückel limiting slope for apparent molar isentropic compressibility, and the slope $B_k$ is an empirical constant obtained by fitting. The values of $k_\phi^0$ for the m2HEAPr in water were determined using least-squares fits to the linear plots of $k_\phi - A_k(m)^{1/2}$ versus molality, using the apparent molar isentropic compressibility values listed at table 3 in the range ($m < 6$ mol $\cdot$ kg$^{-1}$), where the mentioned difference follows almost a linear behaviour on molality as well as in dilute electrolyte solutions. The $A_k$ values used at the different temperatures were the recommended ones by Archer and Wang [85], and are given in table 7. In the same table, the limiting values$k_\phi^0$, and the slopes $B_k$ of equation (26) are also given.

The apparent molar isentropic compressibilities were also well described by rational functions (equation (27)):

$$k_\phi = k_\phi^0(T) + \frac{A_k(T)(m)^{1/2} + B_k(T)m}{1 + C_k(T)m}, \quad (27)$$

where $k_\phi^0 = k_0 + k_1 T$, $A_k(T) = a_{k0} + a_{k1}T$, $B_k(T) = b_{k0} + b_{k1}T$, $C_k(T) = c_{k0} + c_{k1}T$.

For dilute IL solutions when ($m \to 0$), equation (27) leads to equation (26). From least squares, the parameters (corresponding to $10^{14}k_\phi$) are $k_0 = -36.5601$ m$^3 \cdot$ mol$^{-1} \cdot$ Pa$^{-1}$, $k_1 = 0.1122$ m$^3 \cdot$ mol$^{-1} \cdot$ Pa$^{-1} \cdot$ K$^{-1}$, $a_{k0} = 7.5283$ m$^3 \cdot$ mol$^{-3/2} \cdot$ kg$^{1/2} \cdot$ Pa$^{-1}$, $a_{k1} = -0.02521$ m$^3 \cdot$ mol$^{-3/2} \cdot$ kg$^{1/2} \cdot$ Pa$^{-1} \cdot$ K$^{-1}$, $b_{k0} = 6.2367$ m$^3 \cdot$ mol$^{-2} \cdot$ kg $\cdot$ Pa$^{-1}$, $b_{k1} = -0.01583$ m$^3 \cdot$ mol$^{-2} \cdot$ kg $\cdot$ Pa$^{-1} \cdot$ K$^{-1}$, $c_{k0} = 0.2521$ kg $\cdot$ mol$^{-1}$, $c_{k1} = -1.9060 \cdot 10^{-4}$ kg $\cdot$ mol$^{-1} \cdot$ K$^{-1}$ and the standard deviation is 0.09 m$^3 \cdot$ mol$^{-1} \cdot$ Pa$^{-1}$. The values of $k_\phi$ calculated from equation (27) are represented in figure 7 as well as the values for 2HEAA calculated by Álvarez *et al.* [59], for comparison purpose.

As the limiting apparent molar volumes, the limiting molar apparent compressibility, $k_\phi^0$, ($k_\phi(x_{IL} \to 0)$), gives the extent of (ion + solvent) interactions. The $k_\phi^0$ values are appreciably negative for m2HEAPr and 2HEAA [59], especially at lower temperatures, indicating that these ILs lead to an electrostriction effect, which means a decrease in the mixture compressibility. The main factors contributing to the $k_\phi^0$ values are the ions intrinsic compressibility (usually a positive contribution), and the penetration of the solvent

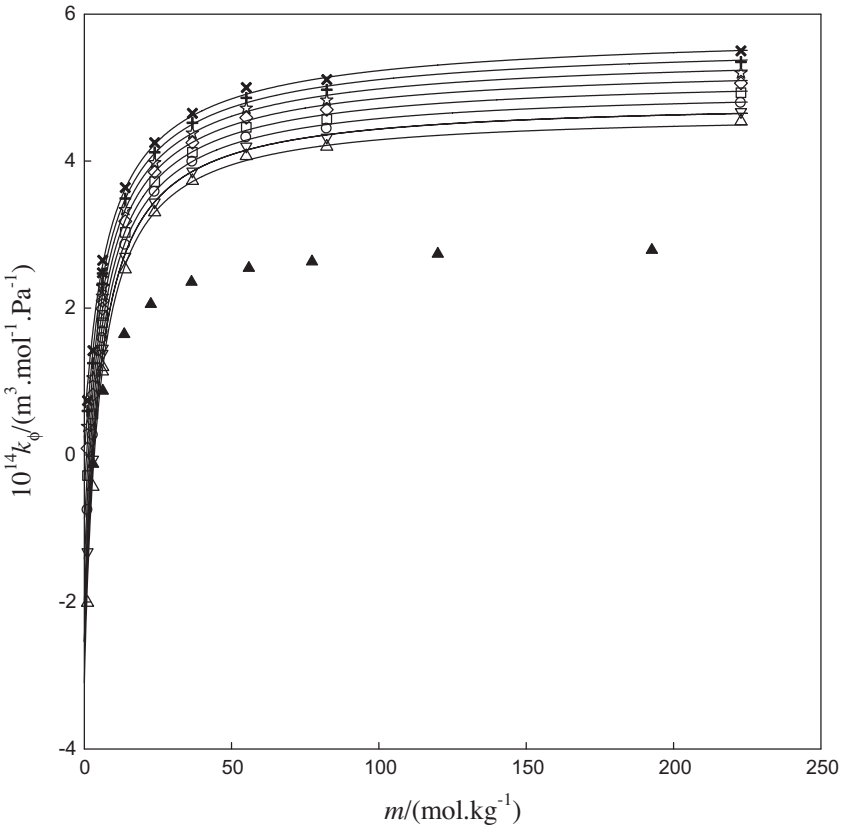


**FIGURE 7.** Apparent molar isentropic compressibility, $k_\phi$, versus molality, $m$, at several temperatures: For {m2HEAPr(1) + $H_2O$(2)}: △, $T = 298.15$ K; ▽, $T = 303.15$ K; ○, $T = 308.15$ K; □, $T = 313.15$ K; ◇, $T = 318.15$ K; ; ☆, $T = 323.15$ K ; +, $T = 328.15$ K, ×, $T = 333.15$ K. Solid curves were calculated from equation (27). ▲, (2HEAA(1) + $H_2O$(2)) at $T = 303.15$ K, [59].

**TABLE 7**
Theoretical Debye–Hückel limiting slope $A_K$ for a 1:1 electrolyte in water, infinite dilution apparent molar isentropic compressibility $k_\phi^0$ and empirical parameters $B_k$ for m2HEAPr in water at several temperatures.

| $T$/K | $10^{14}A_k$ [a]/$m^3 \cdot kg^{1/2} \cdot mol^{-3/2} \cdot Pa^{-1}$ | $10^{14}k_\phi^0$ equation (26)/$m^3 \cdot mol^{-1} \cdot Pa^{-1}$ | $10^{14}k_\phi^0$ equation (27)/$m^3 \cdot mol^{-1} \cdot Pa^{-1}$ | $10^{14}B_k/m^3 \cdot kg \cdot mol^{-2} \cdot Pa^{-1}$ | $\sigma$ equation (26) $m^3 \cdot mol^{-1} \cdot Pa^{-1}$ |
|---|---|---|---|---|---|
| 298.15 | −0.33586 | −2.77 | −3.10 | 0.5073 | 0.23 |
| 303.15 | −0.39045 | −2.10 | −2.54 | 0.4151 | 0.14 |
| 308.15 | −0.45010 | −1.57 | −1.98 | 0.3370 | 0.07 |
| 313.15 | −0.51468 | −1.13 | −1.42 | 0.2747 | 0.04 |
| 318.15 | −0.58427 | −0.81 | −0.86 | 0.2242 | 0.05 |
| 323.15 | −0.65912 | −0.55 | −0.30 | 0.1819 | 0.07 |
| 328.15 | −0.73964 | −0.40 | 0.26 | 0.1529 | 0.08 |
| 333.15 | −0.82634 | −0.33 | 0.83 | 0.1329 | 0.09 |

[a] The values of $A_k$ in reference [85] were expressed in terms of $cm^3 \cdot kg^{1/2} \cdot mol^{-3/2} \cdot MPa^{-1}$.

molecules in the free volume of the ionic solute (negative contribution). Therefore the significant negative $k_\phi^0$ will be due to the predominance of water penetration compared with the compressibility of the ionic species. Zhao *et al.* [94] referred that ILs dilute solutions can form oligomeric aggregates between cations and anions with free volume depending on the solution concentration. This situation will cause penetration of small water molecules in the intra-ionic free space. Furthermore, Álvarez *et al.* [59] studied the aggregation, dynamic behaviour and hydrogen-bond network of aqueous mixtures of 2HEAA by thermo-acoustical, X-ray, and nuclear magnetic resonance techniques. They concluded that a water structure around the ($-NH_3^+$) species exists at different water mole fractions reflecting the transient formation of a complex with a long life between 2HEAA and one or more water molecules.

An important parameter in the study of liquid state is the molar compressibility also called Wada's constant [95] defined by equation (28):

$$k_m = \frac{M}{\rho} k_S^{-1/7}. \tag{28}$$

The molar compressibility is obtained from integration of the differential relationship [96] (equation (29)),

$$\left(\frac{\partial \ln k_s}{\partial T}\right)_P = -7\alpha_p. \tag{29}$$

The results for molar compressibility of pure m2HEAPr and water as well for the mixtures of the two liquids are presented in table 3 and depicted in figure 8 versus temperature for fixed compositions. The uncertainties in the calculation of $k_m$, $u(k_m)$, were estimated as $\pm 3.0 \cdot 10^{-7}\ m^3 \cdot mol^{-1} \cdot Pa^{1/7}$ and $\pm 7.0 \cdot 10^{-7}\ m^3 \cdot mol^{-1} \cdot Pa^{1/7}$ at low and high concentrations of ionic liquid, respectively.

It is clearly observed that $k_m$ is an almost constant function of temperature. Besides, it is observed that $k_m$ is a weak function of temperature. The coefficients $k_1$, $k_2$, and $k_3$, of the representation $k_m = k_1 + k_2T + k_3T^2$ as well as the standard deviations of the fittings are given in table 8. The contribution to $k_m$ of the temperature dependent term is less than 2% except for water and the IL dilute solutions ($x_1 \leqslant 0.1$). As the molar compressibility is slightly temperature dependent, it seems logical to calculate the mean values $\langle k_m \rangle = (1/N_p)\sum_i^{N_p}(k_m)_i$ for each value of mole fraction. These

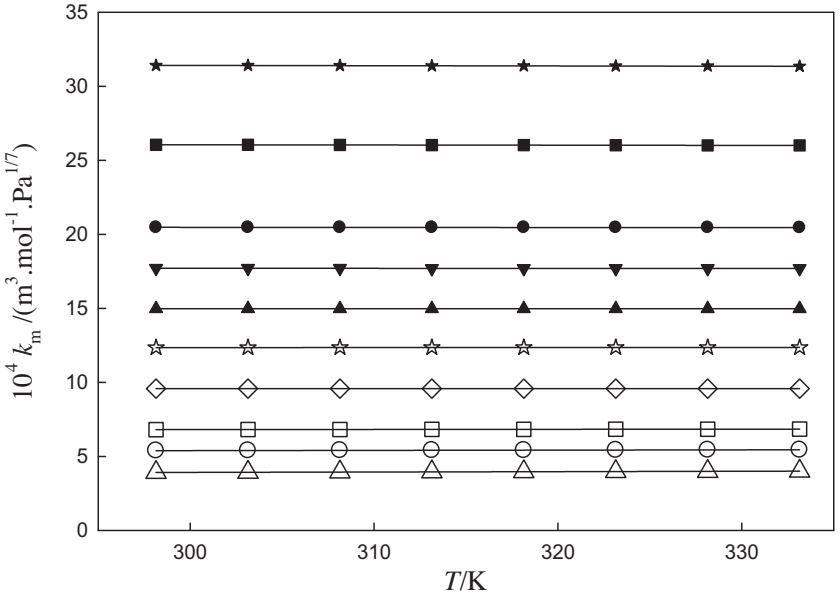


**FIGURE 8.** Molar compressibility of {m2HEAPr(1) + $H_2O$(2)}, $k_m$, as a function of temperature and mole fraction of IL. △, $x_1 = 0$; ○, $x_1 = 0.05$; □, $x_1 = 0.1001$; ◇, $x_1 = 0.2006$; ☆, $x_1 = 0.3010$; ▲, $x_1 = 0.3978$; ▼, $x_1 = 0.4976$; ●, $x_1 = 5972$; ■, $x_1 = 0.8006$; ★, $x_1 = 1.000$. Lines correspond to correlation with a parabolic function on temperature. For iso mole fraction the range of temperature is (298.15 to 333.15) K at 5 K intervals.

**TABLE 8**
Parameters ($k_1$, $k_2$, $k_3$), and standard deviation ($\sigma$) of polynomials equations fitted to the ($k_m$, $T$) data for fixed mole fractions, mean molar compressibility ($\langle k_m \rangle$), standard deviation and average relative deviation from the mean molar compressibility ($\sigma_{km}$ , *AAD*).

| Parameters $x_1$ | $k_1 \cdot 10^4$/ ($m^3 \cdot mol^{-1} \cdot Pa^{1/7}$) | $k_2 \cdot 10^4$/ ($m^3 \cdot mol^{-1} \cdot Pa^{1/7} \cdot K^{-1}$) | $k_3 \cdot 10^4$/ ($m^3 \cdot mol^{-1} \cdot Pa^{1/7} \cdot K^{-2}$) | $\sigma$/ ($m^3 \cdot mol^{-1} \cdot Pa^{1/7}$) | $\langle k_m \rangle \cdot 10^4$/ ($m^3 \cdot mol^{-1} \cdot Pa^{1/7}$) | $\sigma_{km} \cdot 10^4$/ ($m^3 \cdot mol^{-1} \cdot Pa^{1/7}$) | *AAD%* |
|---|---|---|---|---|---|---|---|
| 0.0000 | 3.1694 | $2.4988 \cdot 10^{-3}$ | 0 | $1.2 \cdot 10^{-3}$ | 3.9582 | 0.029 | 0.631 |
| 0.0200 | 3.6154 | $3.0167 \cdot 10^{-3}$ | 0 | $3 \cdot 10^{-4}$ | 4.5676 | 0.035 | 0.660 |
| 0.0501 | 4.8926 | $1.6575 \cdot 10^{-3}$ | 0 | $9 \cdot 10^{-5}$ | 5.4158 | 0.019 | 0.306 |
| 0.1001 | 6.5495 | $8.7289 \cdot 10^{-4}$ | 0 | $5 \cdot 10^{-5}$ | 6.8250 | 0.010 | 0.128 |
| 0.1010 | 6.5679 | $8.9524 \cdot 10^{-4}$ | 0 | $3 \cdot 10^{-4}$ | 6.8505 | 0.010 | 0.131 |
| 0.1921 | 9.0210 | $1.6881 \cdot 10^{-3}$ | 0 | $3 \cdot 10^{-4}$ | 9.5539 | 0.019 | 0.177 |
| 0.2006 | 9.30278 | $1.6554 \cdot 10^{-3}$ | $-2.4936 \cdot 10^{-6}$ | $5.1261 \cdot 10^{-6}$ | 9.5765 | $9.7 \cdot 10^{-4}$ | 0.009 |
| 0.3010 | 11.9429 | $2.2301 \cdot 10^{-3}$ | $-2.9398 \cdot 10^{-6}$ | $6.2209 \cdot 10^{-6}$ | 12.3536 | $4.3 \cdot 10^{-3}$ | 0.030 |
| 0.3978 | 14.5547 | $2.6849 \cdot 10^{-3}$ | $-4.2691 \cdot 10^{-6}$ | $8.9273 \cdot 10^{-6}$ | 14.9763 | $5 \cdot 10^{-4}$ | 0.003 |
| 0.4976 | 17.2173 | $3.3501 \cdot 10^{-3}$ | $-5.7770 \cdot 10^{-6}$ | $1.2381 \cdot 10^{-5}$ | 17.6984 | $3.5 \cdot 10^{-3}$ | 0.017 |
| 0.5972 | 19.9327 | $3.9243 \cdot 10^{-3}$ | $-7.1239 \cdot 10^{-6}$ | $1.5348 \cdot 10^{-5}$ | 20.4607 | $6.6 \cdot 10^{-3}$ | 0.028 |
| 0.8006 | 25.3644 | $5.4676 \cdot 10^{-3}$ | $-1.068 \cdot 10^{-5}$ | $2.4 \cdot 10^{-5}$ | 26.0244 | 0.015 | 0.049 |
| 1.0000 | 31.9226 | $1.7265 \cdot 10^{-3}$ | 0 | $7.3 \cdot 10^{-3}$ | 31.3776 | 0.021 | 0.060 |

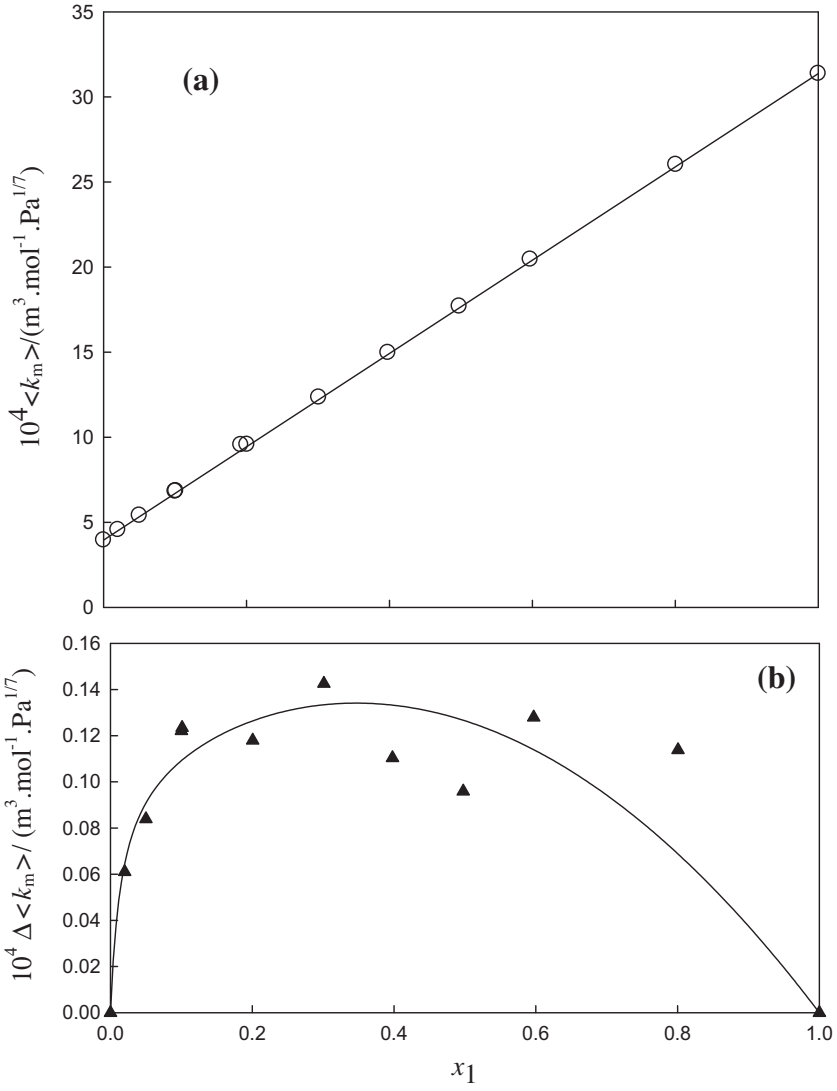


**FIGURE 9.** Mean molar compressibility, $\langle k_m \rangle$, and deviation of mean molar compressibility, $\Delta\langle k_m \rangle$, as a function of mole fraction $x_1$ in aqueous mixtures {m2HEAPr(1) + $H_2O$(2)}. (a) Mean molar compressibility: ○, calculated mean values in the range $T$ = 298.15 K to 333.15 K for each mole fraction; solid line corresponds to $\langle k_m \rangle^*$. (b) Mean molar compressibility deviations: ▲, calculated values from equation (32); solid line corresponds to equation (33).

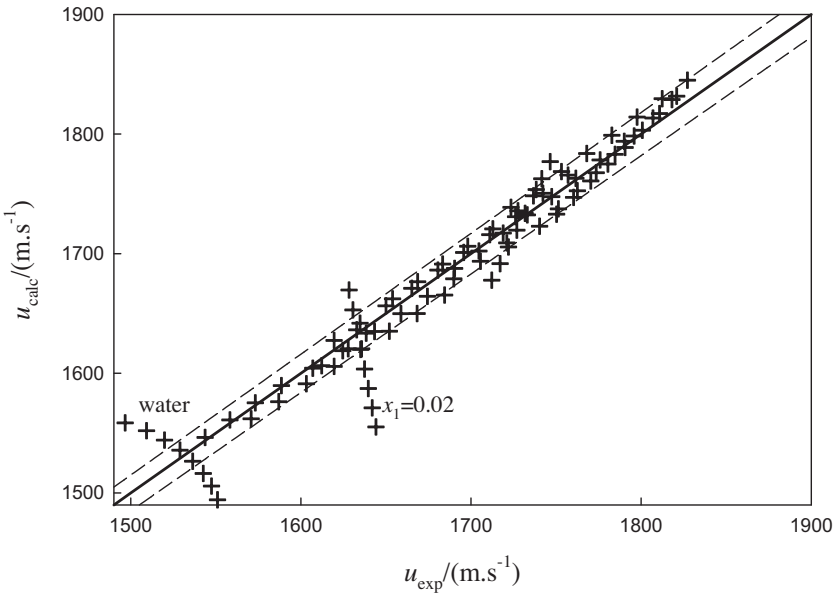


**FIGURE 10.** Parity plot showing the distribution of experimental and calculated values of the speed of sound for {m2HEAPr(1) + $H_2O$(2)} mixtures. Dashed lines refer to ±1% deviation.

values are presented in table 8 as well as the standard deviation from the mean value of molar compressibility, $\sigma_{km}$, and the average absolute deviation from the mean, *AAD*% defined respectively, by equations (30) and (31):

$$\sigma_{km} = \left[\sum_{i=1}^{N_p}(k_m - \langle k_m\rangle)_i^2/N_p\right]^{1/2}, \tag{30}$$

$$AAD\% = (100/N_p)\sum_{i=1}^{N_p}|(k_m - \langle k_m\rangle)/\langle k_m\rangle|_i. \tag{31}$$

The standard deviation $\sigma_{km}$ and the *AAD*% are usually lower than $1\cdot10^{-6}$ m$^3\cdot$mol$^{-1}\cdot$Pa$^{1/7}$ and 0.05%, respectively, except for water and the IL dilute solutions. Thus, it can be concluded that the mean molar compressibility is almost independent on temperature either for pure m2HEAPr and water as well for the mixtures of these components. For the mixture (m2HEAPr + $H_2O$), $\langle k_m\rangle$ will nearly be a linear function on mole fraction of IL as shown in figure 9(a) where the linear term $\langle k_m\rangle^* = x_1\langle k_m\rangle_1 + x_2\langle k_m\rangle_2$ connecting the pure liquid mean molar compressibilities ($\langle k_m\rangle_1$ and $\langle k_m\rangle_2$), was also plotted.

The mean molar compressibility can be described by equation (32):

$$\langle k_m\rangle = \langle k_m\rangle^* + \Delta\langle k_m\rangle. \tag{32}$$

The molar compressibility deviation, $\Delta\langle k_m\rangle$, of the m2HEAPr aqueous mixtures calculated from equation (32) is represented as function of the mole fraction of the m2HEAPr in figure 9(b). The deviation values are small but they cannot be neglected in the $\langle k_m\rangle$ calculation. They may be conveniently represented by the function described in equation (33):

$$\Delta\langle k_m\rangle = x_1x_2\frac{A}{1+B(2x_1-1)}, \tag{33}$$

where the parameters $A = 0.4562$ m$^3\cdot$mol$^{-1}\cdot$Pa$^{1/7}$ and $B = 0.8155$ were found by fitting equation (33) to $\Delta\langle k_m\rangle$ values. The mean $\langle k_m\rangle$ is almost independent on temperature, for fixed mole fraction, and it is only dependent on composition. Thus, the speed of sound of an aqueous mixture can be predicted at any temperature and composition using the equation (34):

$$u = (\langle k_m\rangle/M)^{7/2}\cdot\rho^3 \tag{34}$$

obtained from equation (28) considering $k_m = \langle k_m\rangle$ with the mean $\langle k_m\rangle$ calculated from equations (32) and (33) . The experimental and predicted values of $u$ are represented in the parity plot of figure 10. With the exception of pure water and very dilute IL solutions ($x_1 = 0.02$), the deviations between the calculated and experimental $u$ values are less than 1%. The higher deviations for pure water and dilute aqueous solutions of IL at some temperatures are consequence of significant differences between $k_m$ and the temperature averaged value $\langle k_m\rangle$. Also, these differences are related to different behaviour of the density and speed of sound with temperature change. Equations (32)–(34) will be important for future development of acoustical properties correlation and prediction methods in pure ILs and their mixtures with water or other solvents.

## 4. Conclusions

Values of the speed of sound of pure m2HEAPr measured in this study at atmospheric pressure show a variation of (3 to 4)% at $T$ = (293.15 and 338.15) K, when compared to the data from the literature. The Wu *et al.* equation predicts the measured values with a maximum deviation of +2% at $T$ = 343.15 K.

The excess molar volume, excess isentropic compressibility, molar compressibility, apparent molar volume and apparent molar isentropic compressibility for the binary mixtures (m2HEAPr + water) were calculated from the measured density and speed of sound at temperatures over the range (298.15 to 333.15) K over the whole compositions range.

The analytical representation of (IL + water) mixtures density can be made with reasonable accuracy with Jouyban–Acree model and an optimal representation is achieved through the use of rational functions on temperature and IL mole fraction. For all systems, $V_m^E$ and $k_S^E$ show appreciable negative values. The binary $V_m^E$ and $k_S^E$ values were correlated successfully by using rational functions with a minimum number of coefficients. The $k_S^E$ curves *vs* mole fraction showed a remarkable asymmetry, with their minima toward to the rich compositions in water. This behaviour indicates

the presence of (ion + dipole) interactions and packing between water and ionic liquid.

The high positive values of the limiting apparent molar volumes indicate appreciable (ion + solvent) interactions when the IL is added to water with hydrogen bonding between water and the methyl-hydroxyethyl ammonium cation. The negative apparent molar isentropic compressibility at lower temperatures could indicate that in aqueous m2HEAPr mixtures there will be important penetration of water in the ionic structure.

For (m2HEAPr+water), the molar compressibility calculated from Wada's model is almost a linear function of mole fraction and can be considered as temperature independent for a fixed mole fraction in the whole composition range.

## Acknowledgments

This research is sponsored by FEDER funds through the program COMPETE – Operational Programme for Competitiveness Factors – and by national funds through FCT – Foundation for the Science and Technology, under the project PEst-C/EME/UI0285/2013. P.J. Carvalho acknowledge FCT for their post-doctoral grant SFRH/BD/41562/2007. S. Mattedi acknowledges CNPq/MCT/Brazil (Grant 306560/2013-5 and project 455773/2012-2).

## References

[1] K.M. Docherty, C.F. Kulpa, Green Chem. 7 (2005) 185–189.
[2] D. Zhao, Y. Liao, Z. Zhang, Clean 35 (2007) 42–48.
[3] J. Ranke, A. Muller, U. Bottin-Weber, F. Stock, S. Stolte, J. Arning, R. Stormann, B. Jastorff, Ecotoxicol. Environ. Safe. 67 (2007) 430–438.
[4] X. Yuan, S. Zhang, J. Liu, X. Lu, Fluid Phase Equilib. 257 (2007) 195–200.
[5] M. Iglesias, A. Torres, R. Gonzalez-Olmos, D. Salvatierra, J. Chem. Thermodyn. 40 (2008) 119–133.
[6] N.M.C. Talavera-Prieto, A.G.M. Ferreira, P.N. Simões, P.J. Carvalho, S. Mattedi, J.A.P. Coutinho, J. Chem. Thermodyn. 68 (2014) 221–234.
[7] J. Sierra, E. Martí, A. Mengíbar, R. González-Olmos, M. Iglesias, R. Cruañas, M.A. Garau, Effect of new ammonium based ionic liquids on soil microbial activity, 5th Society of Environmental Toxicology and Chemistry Congress, Sydney, 2008.
[8] L.M. Varela, M. Garcia, F. Sarmiento, D. Attwood, V. Mosquera, J. Chem. Phys. 107 (1997) 6415–6419.
[9] I.B. Malham, P. Letellier, A. Mayaffre, M. Turmine, J. Chem. Thermodyn. 39 (2007) 1132–1143.
[10] J.A. Widegren, J.W. Magee, J. Chem. Eng. Data 52 (2007) 2331–2338.
[11] L. Gaillon, J. Sirieix-Plenet, P. Letellier, J. Sol. Chem. 33 (2004) 1333–1347.
[12] X.-M. Lu, W.-G. Xu, J.-S. Gui, H.-W. Li, J.-Z. Yang, J. Chem. Thermodyn. 37 (2005) 13–19.
[13] M.T. Zafarani-Moattar, H. Shekaari, J. Chem. Thermodyn. 37 (2005) 1029–1035.
[14] A.V. Orchillés, V. González-Alfaro, P.J. Miguel, E. Vercher, A. Martínez-Andreu, J. Chem. Thermodyn. 38 (2006) 1124–1129.
[15] W. Liu, T. Zhao, Y. Zhang, H. Wang, M. Yu, J. Solution Chem. 35 (2006) 1337–1346.
[16] R.L. Gardas, D.H. Dagade, S.S. Terdale, J.A.P. Coutinho, K.J. Patil, J. Chem. Thermodyn. 40 (2008) 695–701.
[17] H. Shekaari, E. Armanfar, J. Chem. Eng. Data 55 (2010) 765–772.
[18] K.R. Seddon, A. Stark, M.J. Torres, Pure Appl. Chem. 72 (2000) 2275–2287.
[19] J.J. Galán, J.L. Castillo, A. González-Pérez, J. Czapkiewicz, J.R. Rodríguez, J. Solution Chem. 32 (2003) 919–927.
[20] B.D. Fitchett, T.N. Knepp, J.C. Conboy, J. Electrochem. Soc. 151 (2004) E219.
[21] S. Pandey, K.A. Fletcher, S.N. Baker, G.A. Baker, Analyst 129 (2004) 569–573.
[22] J.A. Widegren, A. Laesecke, J.W. Magee, Chem. Commun. (2005) 1610–1612.
[23] D. Chakrabarty, A. Chakraborty, D. Seth, N. Sarkar, J. Phys. Chem. A 109 (2005) 1764–1769.
[24] R.L. Gardas, M.G. Freire, P.J. Carvalho, I.M. Marrucho, I.M.A. Fonseca, A.G.M. Ferreira, J.A.P. Coutinho, J. Chem. Eng. Data 52 (2007) 80–88.
[25] M.G. Freire, P.J. Carvalho, A.M. Fernandes, I.M. Marrucho, A.J. Queimada, J.A.P. Coutinho, J. Colloid Interf. Sci. 314 (2007) 621–630.
[26] J. Jacquemin, P. Husson, A.A.H. Padua, V. Majer, Green Chem. 8 (2006) 172–180.
[27] J.-Z. Yang, J.-B. Li, J. Tong, M. Hong, Acta Chim. Sin. 65 (2007) 655–659.
[28] J.S. Torrecilla, T. Rafione, J. García, F. Rodríguez, J. Chem. Eng. Data 53 (2008) 923–928.
[29] W. Liu, L. Cheng, Y. Zhang, H. Wang, M. Yu, J. Mol. Liq. 140 (2008) 68–72.
[30] B. Wu, Y.M. Zhang, H.P. Wang, J. Chem. Eng. Data 54 (2009) 1430–1434.
[31] L. Dong, D.X. Zheng, Z. Wei, X.H. Wu, Int. J. Thermophys. 30 (2009) 1480–1490.
[32] A. Stoppa, J. Hunger, R. Buchner, J. Chem. Eng. Data 54 (2009) 472–479.
[33] S. Zhang, X. Li, H. Chen, J. Wang, J. Zhang, M. Zhang, J. Chem. Eng. Data 49 (2004) 760–764.
[34] L.P.N. Rebelo, V. Najdanovic-Visak, Z.P. Visak, M. Nunes da Ponte, J. Szydlowski, C.A. Cerdeirina, J. Troncoso, L. Romani, J.M.S.S. Esperancua, H.J.R. Guedes, H.C.A. Sousa, Green Chem. 6 (2004) 369–381.
[35] H. Xu, D. Zhao, P. Xu, F. Liu, G. Gao, J. Chem. Eng. Data 50 (2005) 133–135.
[36] J.-Z. Yang, X.-M. Lu, J.-S. Gui, W.-G. Xu, H.-W. Li, J. Chem. Thermodyn. 37 (2005) 1250–1255.
[37] E. Gomez, B. Gonzalez, A. Dominguez, E. Tojo, J. Tojo, J. Chem. Eng. Data 51 (2006) 696–701.
[38] A. Jarosik, S.R. Krajewski, A. Lewandowski, P. Radzimski, J. Mol. Liq. 123 (2006) 43–50.
[39] Q. Zhou, L.-S. Wang, H.-P. Chen, J. Chem. Eng. Data 51 (2006) 905–908.
[40] E. Gomez, B. Gonzalez, N. Calvar, E. Tojo, A. Dominguez, J. Chem. Eng. Data 51 (2006) 2096–2102.
[41] H. Rodriguez, J.F. Brennecke, J. Chem. Eng. Data 51 (2006) 2145–2155.
[42] N. Calvar, B. Gonzalez, A. Dominguez, J. Tojo, J. Solution Chem. 35 (2006) 1217–1225.
[43] Q. Zhou, L.S. Wang, H.P. Chen, J. Chem. Eng. Data 51 (2006) 905–908.
[44] Q.G. Zhang, F. Xue, J. Tong, W. Guan, B. Wang, J. Solution Chem. 35 (2006) 297–309.
[45] J. Vila, P. Ginés, E. Rilo, O. Cabeza, L.M. Varela, Fluid Phase Equilib. 247 (2006) 32–39.
[46] E. Vercher, A.V. Orchillés, P.J. Miguel, A. Martinez-Andreu, J. Chem. Eng. Data 52 (2007) 1468–1482.
[47] E. Gómez, B. González, N. Calvar, A. Domínguez, J. Chem. Thermodyn. 40 (2008) 1208–1216.
[48] N. Calvar, E. Gómez, B. González, A. Domínguez, J. Chem. Eng. Data 52 (2007) 2529–2535.
[49] B. González, N. Calvar, E. Gómez, J. Chem. Thermodyn. 40 (2008) 1274–1281.
[50] J. Ortega, R. Vreekamp, E. Penco, E. Marrero, J. Chem. Thermodyn. 40 (2008) 1087–1094.
[51] E. Rilo, J. Pico, S. García-Garabal, L.M. Varela, O. Cabeza, Fluid Phase Equilib. 285 (2009) 83–89.
[52] G. García-Miaja, J. Troncoso, L. Romaní, J. Chem. Thermodyn. 41 (2009) 161–166.
[53] B. Mokhtarani, A. Sharifi, H.R. Mortaheb, M. Mirzaei, M. Mafi, F. Sadeghian, J. Chem. Thermodyn. 41 (2009) 323–329.
[54] M.L. Ge, X.G. Ren, Y.J. Song, L.S. Wang, J. Chem. Eng. Data 54 (2009) 1400–1402.
[55] E. Rilo, A.G.M. Ferreira, I.M.A. Fonseca, O. Cabeza, Fluid Phase Equilib. 296 (2010) 53–59.
[56] Q. Yang, H. Zhang, B. Su, Y. Yang, Q. Ren, H. Xing, J. Chem. Eng. Data 55 (2010) 1750–1754.
[57] M. Królikowska, P. Lipiński, M. Maik, Thermochim. Acta 582 (2014) 1–9.
[58] U. Domanska, M. Królikowska, J. Solution Chem. 41 (2012) 1422–1445.
[59] V.H. Alvarez, S. Mattedi, M. Martin-Pastor, M. Aznar, M. Iglesias, J. Chem. Thermodyn. 43 (2011) 997–1010.
[60] K.A. Kurnia, M.M. Taib, M.I.A. Mutalib, T. Murugesan, J. Mol. Liq. 159 (2011) 211–219.
[61] K.A. Kurnia, M.I.A. Mutalib, T. Murugesan, B. Ariwahjoedi, J. Solution Chem. 40 (2011) 818–831.
[62] K.A. Kurnia, B. Ariwahjoedi, M.I.A. Mutalib, T. Murugesan, J. Solution Chem. 40 (2011) 470–480.
[63] M.M. Taib, T. Murugesan, J. Chem. Eng. Data 55 (2010) 5910–5913.
[64] O. Cabeza, S. García-Garabal, L. Segade, M. Domínguez-Pérez, E. Rilo, L.M. Varela, Physical properties of binary mixtures of ILs with water and ethanol. A review, in: Alexander Kokorin (Ed.), Ionic Liquids: Theory, Properties, New Approaches, InTech, 2011, ISBN 978-953-307-349-1, http://dx.doi.org/10.5772/14848. <http://www.intechopen.com/books/ionic-liquids-theory-properties-new-approaches/physical-properties-of-binary-mixtures-of-ils-with-water-and-ethanol-a-review>.
[65] C.E. Ferreira, M.C. Talavera-Prieto, I.M.A. Fonseca, A.T.G. Portugal, A.G.M. Ferreira, J. Chem. Thermodyn. 47 (2012) 183–196.
[66] A.F.G. Lopes, M.C. Talavera-Prieto, A.G.M. Ferreira, J.B. Santos, M.J. Santos, A.T.G. Portugal, Fuel 116 (2014) 242–254.
[67] <http://webbook.nist.gov/chemistry/fluid/> (accessed July 2014).
[68] T.C. Chen, R.A. Fine, F.J. Millero, J. Chem. Phys. 66 (1977) 2142–2144.
[69] V.H. Álvarez, N. Dosil, R. Gonzalez-Cabaleiro, S. Mattedi, M. Martin-Pastor, M. Iglesias, J.M. Navaza, J. Chem. Eng. Data 55 (2010) 625–632.
[70] A. Jouyban, A. Fathi-Azarbayjani, M. Khoubnasabjafari, W.E. Acree, Indian J. Chem. 44A (2005) 1–8.
[71] A. Jouyban, S.H. Maljaei, M. Khoubnasabjafari, A. Fathi-Azarbayjani, W.E. Acree, Indian J. Chem. 51A (2012) 695–698 (40,41).
[72] A. Jouyban, Int. J. Pharm. Pharm. Sci. 11 (2008) 32–57.
[73] R.M. Pires, H.F. Costa, A.G.M. Ferreira, Isabel M.A. Fonseca, J. Chem. Eng. Data 52 (2007) 1240–1245.
[74] O. Redlich, D.M. Meyer, Chem. Rev. 64 (1964) 221–227.
[75] K.S. Pitzer, Activity Coefficients in Electrolyte Solutions, second ed., CRC Press, Boca Raton, 1991.
[76] Y. Marcus, G. Hefter, J. Solution Chem. 28 (1999) 575–592.
[77] J. Ananthaswamy, G. Atkinson, J. Chem. Eng. Data 29 (1984) 81–87.
[78] Y. Marcus, G. Hefter, Chem. Rev. 104 (2004) 3405–3452.
[79] L.M. Pinheiro, A.R.T. Calado, J.C.R. Reis, C.A.N. Viana, J. Solution Chem. 32 (2003) 41–52.
[80] U. Saha, B. Das, J. Chem. Eng. Data 47 (1997) 227–229.
[81] A. Pal, S. Kumar, Z. Phys, Chem 219 (2004) 1169–1186.

[82] J.F. Côté, J.E. Desnoyers, J.C. Justice, J. Solution Chem. 25 (1996) 113–134.
[83] "Recommended Reference Materials For Realization Of Physiochemical Properties", (Recommendations 1976), Editor: K.N. Marsh,IUPAC, Physical Chemistry Division , And Commission on Physiochemical Measurements and Standards*, [SECTION: PERMITTIVITY], COLLATORS: H. KIENITZ & K. N. MARSH, Pure & Appl. Chem., vol. 53, pp.1847—1862.
[84] J.T. Kindt, C.A. Schmuttenmaer, J. Phys. Chem. 100 (1996) 10373–10379.
[85] D.G. Archer, P. Wang, J. Phys. Chem. Ref. Data 19 (1990) 371–411.
[86] M.R. Rao, J. Chem. Phys. 9 (1941) 682–685.
[87] E.A. Guggenheim, J. Chem. Phys. 13 (1945) 253–261.
[88] J.O. Valderrama, L.A. Forero, R.E. Rojas, Ind. Eng. Chem. Res. 51 (2012) 7838–7844.
[89] K.J. Wu, Q.L. Chen, C.H. He, AIChE J. 60 (2014) 1120–1131.
[90] M.N. Roy, R. Dey, A. Jha, J. Chem. Eng. Data 46 (2001) 1327–1329.
[91] G. Douhéret, M.I. Davis, J.C.R. Reis, M.J. Blandamer, Chem. Phys. Chem. 2 (2001) 148–161.
[92] G.C. Benson, O. Kiyohara, J. Chem. Thermodyn. 11 (1979) 1061–1064.
[93] N.C. Dey, J. Bhuyan, I. Haque, J. Solution Chem. 32 (2003) 547–558.
[94] Y. Zhao, J. Wang, H. Lu, R. Lin, J. Chem. Thermodyn. 36 (2004) 1–6.
[95] Y. Wada, J. Phys. Soc. Jpn. 4 (1949) 280–283.
[96] S.S. Mathur, P.N. Gupta, S.C. Sinhat, J. Phys. A: Gen. Phys. 4 (1971) 434–436.

JCT 14-669